

Stability of periodic orbits in no-slip billiards

C. Cox*, R. Feres*, H.-K. Zhang†

November 16, 2018

Abstract

Rigid bodies collision maps in dimension two, under a natural set of physical requirements, can be classified into two types: the standard specular reflection map and a second which we call, after Broomhead and Gutkin, *no-slip*. This leads to the study of *no-slip billiards*—planar billiard systems in which the moving particle is a disc (with rotationally symmetric mass distribution) whose translational and rotational velocities can both change at each collision with the boundary of the billiard domain.

In this paper we greatly extend previous results on boundedness of orbits (Broomhead and Gutkin) and linear stability of periodic orbits for a Sinai-type billiard (Wojtkowski) for no-slip billiards. We show among other facts that: (i) for billiard domains in the plane having piecewise smooth boundary and at least one corner of inner angle less than π , no-slip billiard dynamics will always contain elliptic period-2 orbits; (ii) polygonal no-slip billiards always admit small invariant open sets and thus cannot be ergodic with respect to the canonical invariant billiard measure; (iii) the no-slip version of a Sinai billiard must contain linearly stable periodic orbits of period 2 and, more generally, we provide a curvature threshold at which a commonly occurring period-2 orbit shifts from being hyperbolic to being elliptic; (iv) finally, we make a number of observations concerning periodic orbits in a class of polygonal billiards.

1 INTRODUCTION AND MAIN RESULTS

No-slip billiard systems have received so far very little attention despite some interesting features that distinguish them from the much more widely studied standard billiards. These non-standard types of billiards are discrete time systems in dimension 4 (after taking the natural Poincaré section of a flow) representing a rotating disc with unit kinetic energy that moves freely in a billiard domain with piecewise smooth boundary. Although not Hamiltonian, these systems are nevertheless time reversible and leave invariant the canonical billiard measure. They also exhibit dynamical behavior that is in sharp contrast with standard billiards. For example, they very often contain period-2 orbits having small elliptic islands. These regions exist amid chaos that appears, in numerical experiments, to result from the usual mechanisms of dispersing and focusing.

*Department of Mathematics, Washington University, Campus Box 1146, St. Louis, MO 63130

†Department of Mathematics, University of Massachusetts in Amherst

We are aware of only two articles on this subject prior to our [7, 8]: one by Broomhead and Gutkin [2] showing that no-slip billiard orbits in an infinite strip are bounded, and another by Wojtkowski, characterizing linear stability for a special type of period-2 orbit. In this paper we extend their results as will be detailed shortly, and develop the basic theory of no-slip billiards in a more systematic way. In this section we explain the organization of the paper and highlight our main new results.

Section 2 gives preliminary information and sets notation and terminology concerning rigid collisions. It specializes the general results from [7] (stated in that paper in arbitrary dimension for bodies of general shapes and mass distributions) to discs in the plane with rotationally symmetric mass distributions. The main fact is briefly summarized in Proposition 2.1. Although the classification into specular and no-slip collisions is the same as in [2], our approach is more differential geometric in style and may have some conceptual advantages. For example, we derive this classification (in [7]) from an orthogonal decomposition of the tangent bundle TM restricted to the boundary ∂M (orthogonal relative to the kinetic energy Riemannian metric in the system's configuration manifold M) into physically meaningful subbundles. This orthogonal decomposition is explained here only for discs in the plane.

By a planar *no-slip billiard* system we mean a mechanical system in \mathbb{R}^2 in which one of the colliding bodies, which may have arbitrary shape, is fixed in place, whereas the second, moving body is a disc with rotationally symmetric mass distribution; post-collision velocities (translational and rotational) are determined from pre-collision velocities via the no-slip collision map and between consecutive collisions the bodies undergo free motion. Contrary to the standard case, the moving particle's mass distribution influences the collision properties (via an angle parameter which is denoted β throughout the paper). The main definitions and notations concerning no-slip billiard systems, in particular the notions of *reduced phase space*, *velocity phase space*, and the *product*, *eigen*- and *wavefront* frames, are introduced in Section 3.

A special feature of no-slip billiards around which much of the present study is based, is the ubiquitous occurrence of period-2 trajectories. The general description of these trajectories is given in Section 4. In Section 5 we obtain the differential of the no-slip billiard map and show the form it takes for period-2 trajectories.

For general collision systems as considered in [7] (satisfying energy and momenta conservation, time reversibility, involving impulsive forces that can only act at the contact point between colliding bodies), the issue of characterizing smooth invariant measures still needs much further investigation, although it is shown there that the canonical (Liouville) measure is invariant if a certain field of subspaces defined in terms of the collision maps at each collision configuration $q \in \partial M$ is parallel with respect to the kinetic energy metric. This is the case for planar no-slip billiards, so that the standard billiard measure is still invariant. (Note, however, that the configuration manifold is now 3-dimensional.) A detailed proof of this fact, in addition to comments on time reversibility are given in Section 6.

Dynamics proper begins with Sections 7 and 8, which are concerned with no-slip billiard systems in wedge-shaped regions and polygons. Here we generalize the main result from [2]. In that paper it is shown that orbits of the no-slip billiard system in an infinite strip domain are bounded. By extending and refining this fact to wedge regions we obtain

local stability for periodic orbits in no-slip polygonal billiards. This is Theorem 8.1. We also give in Section 8 an exhaustive description of periodic orbits in wedge billiards.

Finally, in Section 9 we consider linear stability of period-2 orbits in the presence of curvature. Our results here extend those of [16] for no-slip Sinai billiards. Wojtkowski makes in [16] the following striking observation: for a special period-2 orbit in a Sinai billiard (corresponding in our study to angle $\phi = 0$) there is a parameter defined in terms of the curvature of the circular scatterer that sets a threshold between elliptic and hyperbolic behavior. This is based on an analysis of the differential of the billiard map at the periodic trajectory. Here we derive similar results for period-2 orbits in general. Although the analysis is purely linear, we observe the occurrence of elliptic islands and stable behavior in systems that are the no-slip counterpart of fully chaotic standard billiards. The fast transition between stability and chaos near the threshold set by the curvature parameter obtained from the linear analysis is also very apparent numerically. As already observed by Wojtkowski in [16], proving local stability in the presence of curvature would require a difficult KAM analysis (for reversible, but not Hamiltonian systems; cf. [14]).

2 BACKGROUND ON RIGID COLLISIONS

For a much more general treatment of the material of this section (not restricted to discs and valid in arbitrary dimension) see [7]. See also [2, 16]. Let $x = (x_1, x_2)$ be the standard coordinates in \mathbb{R}^2 . A mass distribution on a body $B \subset \mathbb{R}^2$ is defined by a finite positive measure μ_{mass} on $B \subset \mathbb{R}^2$. We assume without loss of generality that the first moments $\int_B x_i d\mu_{\text{mass}}(x)$ vanish. Let m be the total mass: $m = \mu_{\text{mass}}(B)$. The second moments of μ_{mass} (divided by m) will be denoted by $\ell_{rs} = \frac{1}{m} \int_B x_r x_s d\mu_{\text{mass}}(x)$. When B is a disc of radius R centered at the origin of \mathbb{R}^2 , it will be assumed that μ_{mass} is rotationally symmetric, in which case the symmetric matrix $L = (\ell_{rs})$ is scalar: $L = \lambda I$. Also in this case, $0 \leq \lambda \leq R^2/2$, where 0 corresponds to all mass being concentrated at the origin and the upper bound corresponds to having all mass concentrated on the circle of radius R . For the uniform mass distribution, $\lambda = R^2/4$. It will be useful to introduce the parameter $\gamma := \sqrt{2\lambda}/R$. The moment of inertia of a disc of radius R is given in terms of γ by $\mathcal{I} = m(\gamma R)^2$. For the uniform mass distribution on the ball $\gamma = 1/\sqrt{2}$. In general, $0 \leq \gamma \leq 1$.

From now on B will be the disc of radius R in \mathbb{R}^2 centered at the origin. A *configuration* of the moving disc is an image of B under a Euclidean isometry; it is parametrized by the coordinates of the center of mass (y, z) of the image disc and its angle of orientation θ . Introducing the new coordinate $x := \gamma R\theta$ and denoting by $v = (\dot{x}, \dot{y}, \dot{z})$ the velocity vector in configuration space, the kinetic energy of the body takes the form $\frac{1}{2}m|v|^2$, where $|v|$ is the standard Euclidean norm.

We consider now a system of two discs with radii R_1, R_2 , denoted by B_1, B_2 when in their reference configuration, that is, when centered at the origin of \mathbb{R}^2 . The configuration manifold M of the system, which is the set of all non-overlapping images of B_i under Euclidean isometries of the plane, is then the set

$$M := \{(a_1, a_2) \in (\mathbb{R}^2 \times \mathbb{T}_1) \times (\mathbb{R}^2 \times \mathbb{T}_2) : |\bar{a}_1 - \bar{a}_2| \geq R_1 + R_2\},$$

where $\mathbb{T}_i = \mathbb{R}/(2\pi\gamma_i R_i)$ and \bar{a} indicates the coordinate projection of a in \mathbb{R}^2 . Given mass distributions μ_i , $i = 1, 2$, the kinetic energy of the system at a state (a_1, v_1, a_2, v_2) is $K = \frac{1}{2} (m_1 |v_1|^2 + m_2 |v_2|^2)$. The manifold M becomes a Riemannian manifold with boundary by endowing it with the *kinetic energy metric*

$$\langle (u_1, u_2), (v_1, v_2) \rangle = m_1 u_1 \cdot v_1 + m_2 u_2 \cdot v_2$$

where the dot means ordinary inner product in \mathbb{R}^3 .

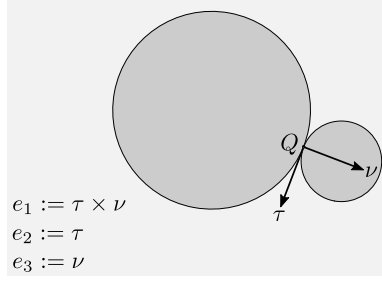


Figure 1: Definition of the (e_1, e_2, e_3) frame at the contact point Q . The unit normal vector ν points away from the center of (the image in the given configuration of) body B_1 .

Let τ and ν denote the unit tangent and normal vectors at the contact point $Q \in \mathbb{R}^2$ of the bodies in a boundary configuration $q \in \partial M$ as indicated in Figure 1. We introduce the orthonormal frame e_1, e_2, e_3 of \mathbb{R}^3 as defined in the figure. If the system is at a state (a_1, v_1, a_2, v_2) , then Q will have velocity $V_i(Q)$ when regarded as a point in body B_i in the given configuration a_i . One easily obtains

$$V_1(Q) = [v_1 \cdot e_2 - \gamma_1^{-1} v_1 \cdot e_1] e_2 + v_1 \cdot e_3 e_3, \quad V_2(Q) = [v_2 \cdot e_2 - \gamma_2^{-1} v_2 \cdot e_1] e_2 + v_2 \cdot e_3 e_3.$$

The unit normal vector to ∂M at the configuration $q = (a_1, a_2)$ pointing towards the interior of M will be denoted \mathfrak{n}_q . Note that this is defined with respect to the kinetic energy metric. Explicitly, letting $m = m_1 + m_2$,

$$\mathfrak{n}_q = \left(-\sqrt{\frac{m_2}{m_1 m}} e_3, \sqrt{\frac{m_1}{m_2 m}} e_3 \right).$$

We also define the *no-slip* subspace \mathfrak{S}_q of the tangent space to ∂M at q :

$$\mathfrak{S}_q = \{ (v_1, v_2) : V_1(Q) = V_2(Q) \},$$

and the orthogonal complement to \mathfrak{S}_q in $T_q \partial M$, which we write as $\bar{\mathfrak{C}}_q$. The orthogonal direct sum of the latter and the line spanned by \mathfrak{n}_q was denoted by \mathfrak{C}_q in [7] and called the *impulse* subspace. These two spaces are given by

$$(2.1) \quad \bar{\mathfrak{C}}_q = \left\{ \left(-\frac{1}{\gamma_1} v_1 \cdot e_2, v_1 \cdot e_2, 0; \frac{1}{\gamma_2} v_2 \cdot e_2, v_2 \cdot e_2, 0 \right) : m_1 v_1 + m_2 v_2 = 0 \right\}$$

and

$$(2.2) \quad \mathfrak{S}_q = \left\{ (v_1, v_2) : (v_1 - v_2) \cdot e_3 = 0, (v_1 - v_2) \cdot e_2 = \left(\frac{v_1}{\gamma_1} + \frac{v_2}{\gamma_2} \right) \cdot e_1 \right\}.$$

Figure 2 shows typical vectors in these orthogonal subspaces.

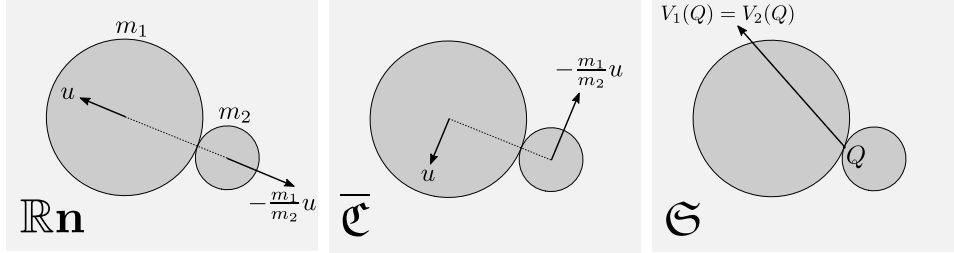


Figure 2: Tangent vectors in $T_q M$ decompose orthogonally (relative to the kinetic energy metric) into vectors of the above three types. In the diagram on the left the bodies are not rotating, and in the middle diagram the rotation velocities are determined by the center of mass velocities as given by (2.1).

We can now state in the present very special case one of the main results of [7]. See also [2]. In the interior of M , the motion of the system, in the absence of potential forces, is geodesic relative to the kinetic energy metric. In dimension two this amounts simply to constant linear and angular velocities. For the motion to be fully specified it is necessary to find for any given $v^- = (v_1^-, v_2^-)$ at $q \in \partial M$ such that $\langle v^-, \mathbf{n}_q \rangle < 0$ (representing the bodies' velocities immediately before a collision) a v^+ such that $\langle v^+, \mathbf{n}_q \rangle > 0$ (representing the bodies' velocities immediately after). This correspondence should be given by a map $C_q : v^- \mapsto v^+$. We call such correspondence a *collision map* C_q at $q \in \partial M$.

Proposition 2.1. *Linear collision maps $C_q : T_q M \rightarrow T_q M$ at $q \in \partial M$ describing energy preserving, (linear and angular) momentum preserving, time reversible collisions having the additional property that impulsive forces between the bodies can only act at the single point of contact (denoted by Q above) are given by the linear orthogonal involutions that restrict to the identity map on \mathfrak{S}_q and send \mathbf{n}_q to its negative. Thus C_q is fully determined by its restriction to \mathfrak{C}_q , where it can only be (in dimension 2) the identity or its negative.*

We refer to [7] for a more detailed explanation of this result. The key point for our present purposes is that, in addition to the standard reflection map given by specular reflection with respect to the kinetic energy metric, there is only one (under the stated assumptions) other map, which we refer to as the *no-slip collision map*.

The explicit form of the no-slip collision map C_q can thus be obtained by first decomposing the pre-collision vector v^- according to the orthogonal decomposition $\mathfrak{S}_q \oplus \mathfrak{C}_q$ and then switching the sign of the \mathfrak{C}_q component to obtain v^+ . If Π_q is the orthogonal projection to \mathfrak{C}_q , then $C_q = I - 2\Pi_q$. Setting $[v] = [(v_1, v_2)] := (v_1 \cdot e_1, v_1 \cdot e_2, v_1 \cdot e_3, v_2 \cdot e_1, v_2 \cdot e_2, v_2 \cdot e_3)^t$, the pre- and post-collision velocities are related by $[v^+] = [C_q][v^-]$ where

$$[C_q] = \begin{pmatrix} 1 - \frac{\delta}{m_1 \gamma_1^2} & \frac{\delta}{m_1 \gamma_1} & 0 & -\frac{\delta}{m_1 \gamma_1 \gamma_2} & -\frac{\delta}{m_1 \gamma_1} & 0 \\ \frac{\delta}{m_1 \gamma_1} & 1 - \frac{\delta}{m_1} & 0 & \frac{\delta}{m_1 \gamma_2} & \frac{\delta}{m_1} & 0 \\ 0 & 0 & 1 - \frac{2m_2}{m} & 0 & 0 & \frac{2m_2}{m} \\ -\frac{\delta}{m_2 \gamma_1 \gamma_2} & \frac{\delta}{m_2 \gamma_2} & 0 & 1 - \frac{\delta}{m_2 \gamma_2} & -\frac{\delta}{m_2 \gamma_2} & 0 \\ -\frac{\delta}{m_2 \gamma_1} & \frac{\delta}{m_2} & 0 & -\frac{\delta}{m_2 \gamma_2} & 1 - \frac{\delta}{m_2} & 0 \\ 0 & 0 & \frac{2m_1}{m} & 0 & 0 & 1 - \frac{2m_1}{m} \end{pmatrix}.$$

Here $m = m_1 + m_2$ and $\delta = 2 \left\{ \frac{1}{m_1} \left[1 + \frac{1}{\gamma_1^2} \right] + \frac{1}{m_2} \left[1 + \frac{1}{\gamma_2^2} \right] \right\}^{-1}$. We record two special cases. First suppose that the two discs have the same mass distribution and $\gamma = \gamma_i$. Then

$$[C_q] = \begin{pmatrix} \frac{\gamma^2}{1+\gamma^2} & \frac{\gamma}{1+\gamma^2} & 0 & -\frac{1}{1+\gamma^2} & -\frac{\gamma}{1+\gamma^2} & 0 \\ \frac{\gamma}{1+\gamma^2} & \frac{1}{1+\gamma^2} & 0 & \frac{\gamma}{1+\gamma^2} & \frac{\gamma^2}{1+\gamma^2} & 0 \\ 0 & 0 & 0 & 0 & 0 & 1 \\ -\frac{1}{1+\gamma^2} & \frac{\gamma}{1+\gamma^2} & 0 & \frac{\gamma^2}{1+\gamma^2} & -\frac{\gamma}{1+\gamma^2} & 0 \\ -\frac{\gamma}{1+\gamma^2} & \frac{\gamma^2}{1+\gamma^2} & 0 & -\frac{\gamma}{1+\gamma^2} & \frac{1}{1+\gamma^2} & 0 \\ 0 & 0 & 1 & 0 & 0 & 0 \end{pmatrix}$$

The second case of interest assumes that one body, say B_1 is fixed in place. It makes sense to pass to the limit in which the mass and moment of inertia of B_1 approach infinity and its velocity (which does not change during collision process as a quick inspection of C_q shows) is set equal to 0. In this case only the velocity of B_2 changes and we write $m = m_2, v = v_2, \gamma = \gamma_2$ and $v = v_2$. Then

$$\mathfrak{n}_q = (0, 0, m^{-1/2}), \quad \mathfrak{S}_q = \{(-\gamma s, s, 0) : s \in \mathbb{R}\}, \quad \overline{\mathfrak{C}}_q = \{(s, \gamma s, 0) : s \in \mathbb{R}\}$$

where vectors are expressed in the frame (e_1, e_2, e_3) . The (lower right block of the) matrix $[C_q]$ is now

$$(2.3) \quad [C_q] = \begin{pmatrix} -\frac{1-\gamma^2}{1+\gamma^2} & -\frac{2\gamma}{1+\gamma^2} & 0 \\ -\frac{2\gamma}{1+\gamma^2} & \frac{1-\gamma^2}{1+\gamma^2} & 0 \\ 0 & 0 & -1 \end{pmatrix} = \begin{pmatrix} -\cos \beta & -\sin \beta & 0 \\ -\sin \beta & \cos \beta & 0 \\ 0 & 0 & -1 \end{pmatrix}.$$

As noted earlier, $\gamma = \tan^2(\beta/2)$ can take any value between 0 and 1 (equivalently, $0 \leq \beta \leq \pi/2$) in dimension 2; thus it makes sense to define the angle β as we did above. When the mass distribution is uniform, $\gamma = 1/\sqrt{2}$ and $\cos \beta = 1/3$, $\sin \beta = 2\sqrt{2}/3$. Notice that these expressions still hold regardless of the shape of the fixed body B_1 . In what follows we denote the above 3-by-3 matrix by $\mathcal{C} := [C_q]$.

3 NO-SLIP PLANAR BILLIARDS

We focus attention on the last case indicated at the end of Section 2, which we call a planar no-slip *billiard*: the billiard table is the complement of the fixed body B_1 , now any set in \mathbb{R}^2 with non-empty interior and piecewise smooth boundary, and the billiard ball is the disc B_2 of radius R with a rotationally symmetric mass distribution. The configuration manifold is then the set M consisting of all $q = (\bar{q}, x) \in \mathbb{R}^2 \times \mathbb{T}$ for which the distance between \bar{q} and B_1 is at least R . We define $\mathbb{T} := \mathbb{R}/(2\pi\gamma R)$. The projection $q \mapsto \bar{q}$ maps M onto the *billiard table*, denoted \mathcal{B} . The boundary of M is $\partial\mathcal{B} \times \mathbb{T}$ and the frame $(e_1(q), e_2(q), e_3(q))$ at $q \in \partial M$ is as indicated in Figure 3. We also view this q -dependent frame as the orthogonal map $\sigma_q : \mathbb{R}^3 \rightarrow T_q\mathbb{R}^3$ that sends the standard basis vectors ϵ_i of \mathbb{R}^3 to $e_i(q)$, for $i = 1, 2, 3$. This allows us to write $C_q = \sigma_q \mathcal{C} \sigma_q^{-1}$ for each q .

Due to energy conservation, the norms of velocity vectors are not changed during collision or during the free motion between collisions; we restrict attention to vectors of unit length (in the kinetic energy metric, which agrees with the standard Euclidean metric in \mathbb{R}^3 under the choice of coordinate $x = \gamma R\theta$ for the disc's angle of orientation).

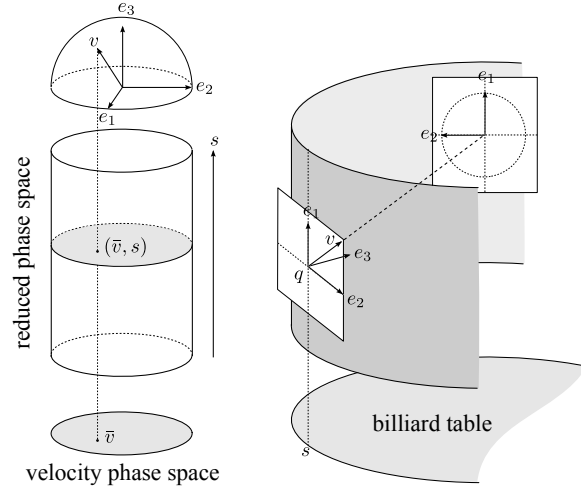


Figure 3: Definition of the product frame (e_1, e_2, e_3) , the reduced phase space, and the velocity phase space.

Throughout the paper the notations $\langle u, v \rangle$ and $u \cdot v$ are both used for the standard inner product in \mathbb{R}^3 , the choice being a matter of typographical convenience. (Recall that the kinetic energy metric has been reduced to the standard inner product in \mathbb{R}^3 by our definition of the variable x .) The *phase space* of the billiard system is

$$N := N^+ := \{(q, v) \in T\mathbb{R}^3 : q \in \partial M, |v| = 1, v \cdot e_3(q) > 0\}.$$

We refer to vectors in N^+ as *post-collision* velocities; we similarly define the space N^- of *pre-collision* velocities. The *billiard map* T , whose domain is a subset of N , is the

composition of the free motion between two points q_1, q_2 in ∂M and the billiard map C_{q_2} at the endpoint. Thus $T : N \rightarrow N$ is given by

$$(\tilde{q}, \tilde{v}) = T(q, v) = (q + tv, C_{\tilde{q}}v)$$

where $t := \inf\{s > 0 : q + sv \in N\}$. (We assume that the shape of the billiard table \mathcal{B} is such that T makes sense and is smooth for all ξ in some big subset of N , say open of full Lebesgue measure.) Let

$$\xi = (q, v) \mapsto \tilde{\xi}_- = (\tilde{q}, v) \mapsto \tilde{\xi} = \tilde{\xi}_+ = (\tilde{q}, C_{\tilde{q}}v).$$

The first map in this composition, which we denote by Φ , is parallel translation of v from q to \tilde{q} , and the second map, denoted C , applies the no-slip reflection map to the translated vector, still denoted v , at \tilde{q} . Hence $T = C \circ \Phi$.

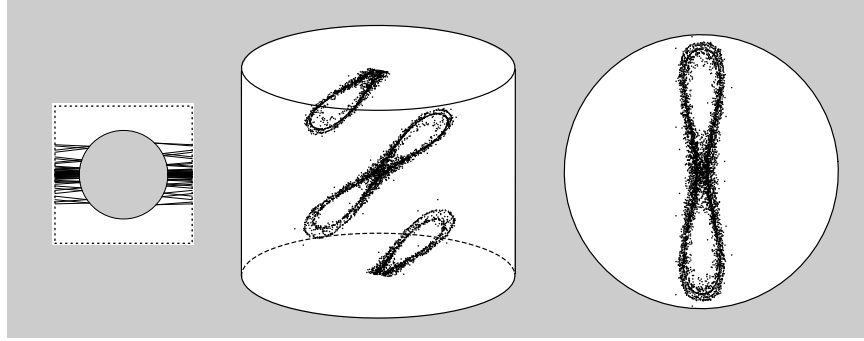


Figure 4: Left: projection from \mathbb{R}^3 to \mathbb{R}^2 of an orbit of the no-slip Sinai billiard, to be discussed in more detail later on. Middle: the same orbit shown in the reduced phase space and, on the right, in the velocity phase space.

Taking into account the rotation symmetry of the moving disc, we may for most purposes ignore the angular coordinate (but not the angular velocity!) and restrict attention to the *reduced phase space*. This is defined as $\partial\mathcal{B} \times \{u \in \mathbb{R}^2 : |u| < 1\}$, where an element u of the unit disc represents the velocity vector at $q \in \partial\mathcal{B}$ (pointing into the billiard region) given by

$$\sigma_q(u_1, u_2, \sqrt{1 - |u|^2}) = u_1 e_1(q) + u_2 e_2(q) + \sqrt{1 - |u|^2} e_3(q).$$

By *velocity phase space* we mean this unit disc. Figure 3 summarizes these definitions and Figure 4 shows what an orbit segment looks like in each space. On the left of the latter figure is shown the two dimensional projection of the orbit segment defined in the 3-dimensional space M .

The rotation symmetry that justifies passing from the 4-dimensional phase space to the 3-dimensional reduced phase space may be formally expressed by the identity

$$T(q + \lambda e_1, v) = T(q, v) + \lambda e_1.$$

Keep in mind that e_1 is a parallel vector field (independent of q). In particular, e_1 is invariant under the differential map: $dT_\xi e_1 = e_1$ for all $\xi = (q, v)$.

In addition to the orthonormal frames σ_q it will be useful to introduce a frame consisting of eigenvectors of the collision map C_q . We define

$$(3.1) \quad \begin{aligned} u_1(q) &= \sin(\beta/2)e_1(q) - \cos(\beta/2)e_2(q) \\ u_2(q) &= \cos(\beta/2)e_1(q) + \sin(\beta/2)e_2(q) \\ u_3(q) &= e_3(q). \end{aligned}$$

See Figure 5. Then

$$C_q u_1(q) = u_1(q), \quad C_q u_2(q) = -u_2(q), \quad C_q u_3(q) = -u_3(q).$$

Yet a third orthonormal frame will prove useful later on in our analysis of period-2 trajectories. Let $\xi = (q, v) \in N$. Then $w_1(\xi), w_2(\xi), w_3(\xi)$ is the orthonormal frame at q such that

$$w_1(\xi) := \frac{e_1(q) - e_1(q) \cdot vv}{|e_1(q) - e_1(q) \cdot vv|}, \quad w_2(\xi) := v \times w_1(\xi), \quad w_3(\xi) := v.$$

Note that $w_1(\xi)$ and $w_2(\xi)$ span the 2-space perpendicular to v .

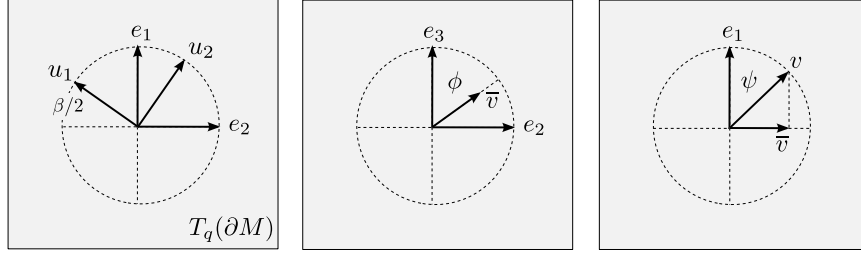


Figure 5: Some angle and frame definitions: the q -dependent product frame $(e_i(q))$, the eigenframe (u_i) for the collision map C_q at a collision configuration $q \in \partial M$, the characteristic angle β (a function of the mass distribution of the disc), and the angles $\phi(q, v)$ and $\psi(q, v)$.

Definition 3.1 (Special orthonormal frames). *For any given $\xi = (q, v) \in N$ we refer to*

$$(e_1(q), e_2(q), e_3(q)), \quad (u_1(q), u_2(q), u_3(q)), \quad (w_1(\xi), w_2(\xi), w_3(\xi))$$

as the product frame, the eigenframe, and the wavefront frame, respectively.

4 PERIOD-2 ORBITS

It appears to be a harder problem in general to show the existence of periodic orbits for no-slip billiards than it is for standard billiard systems in dimension 2, despite numerical

evidence that such points are common. A few useful observations can still be made for specific shapes of \mathcal{B} . We begin here with the general description of period-2 orbits. The reader should bear in mind that, when we represent billiard orbits in figures such as 11, we often draw their projections on the plane, even though periodicity refers to a property of orbits in the 3-dimensional reduced phase space.

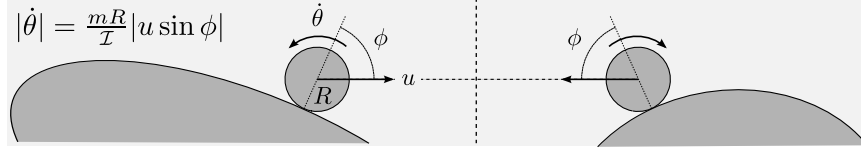


Figure 6: Period 2 orbit. The indicated parameters are: the disc's mass m , its moment of inertia \mathcal{I} , and radius R . The velocity of the center of mass is u and the angular velocity is $\dot{\theta}$.

Let $\xi = (q, v)$ be the initial state of a periodic orbit of period 2, $\tilde{\xi} = (\tilde{q}, \tilde{v}) = T(\xi)$, and t the time of free flight between collisions. Then, clearly,

$$(q, v) = (\tilde{q} + tC_{\tilde{q}}v, C_{\tilde{q}}\tilde{v}) = (q + t(v + C_{\tilde{q}}v), C_qC_{\tilde{q}}v)$$

so that $C_{\tilde{q}}v = -v$ and $v = C_qC_{\tilde{q}}v$. Because v and $u_1(q)$ (respectively, $u_1(\tilde{q})$) are eigenvectors for different eigenvalues of the orthogonal map C_q (respectively, $C_{\tilde{q}}$), v is perpendicular to both $u_1(q)$ and $u_1(\tilde{q})$. It follows from (3.1) that $u_1(q) \cdot e_1 = u_1(\tilde{q}) \cdot e_1$. Thus the projection of e_1 to v^\perp is proportional to $u_1(q) + u_1(\tilde{q})$. By the definition of the wavefront vector $w_1(\xi)$ (and the angle ϕ , cf. Figure 5) we have

$$w_1(\xi) = w_1(\tilde{\xi}) = \frac{u_1(q) + u_1(\tilde{q})}{|u_1(q) + u_1(\tilde{q})|} = \frac{u_1(q) + u_1(\tilde{q})}{2\sqrt{1 - \cos^2(\beta/2) \cos^2 \phi}}.$$

Now observe that $u_1(\tilde{q}) - u_1(q)$ is perpendicular to $u_1(q) + u_1(\tilde{q})$. It follows from this remark and a glance at Figure 5 (to determine the orientation of the vectors) that

$$w_2(\xi) = -w_2(\tilde{\xi}) = \frac{u_1(\tilde{q}) - u_1(q)}{|u_1(\tilde{q}) - u_1(q)|} = \frac{u_1(\tilde{q}) - u_1(q)}{2\cos(\beta/2) \cos \phi}.$$

Notice, in particular, that v is a positive multiple of $u_1(q) \times u_1(\tilde{q})$. An elementary calculation starting from this last observation gives v in terms of the product frame:

$$v = \frac{\cos(\beta/2) \sin \phi e_1 + \sin(\beta/2) [\sin \phi e_2(q) + \cos \phi e_3(q)]}{\sqrt{1 - \cos^2(\beta/2) \cos^2 \phi}}.$$

A more physical description of the velocity v of a period-2 orbit is shown in Figure 6 in terms of the moment of inertia \mathcal{I} .

Equally elementary computations yield the collision map C_q in the wavefront frame at q , for a period-2 state $\xi = (q, v)$. We register this here for later use. To shorten the

equations we write $c_{\beta/2} = \cos(\beta/2)$ and $c_\phi = \cos \phi$.

$$\begin{aligned}
C_q w_1(\xi) &= (1 - 2c_{\beta/2}^2 c_\phi^2) w_1(\xi) - 2c_{\beta/2} c_\phi \sqrt{1 - c_{\beta/2}^2 c_\phi^2} w_2(\xi) \\
C_q w_2(\xi) &= -2c_{\beta/2} c_\phi \sqrt{1 - c_{\beta/2}^2 c_\phi^2} w_1(\xi) - (1 - 2c_{\beta/2}^2 c_\phi^2) w_2(\xi) \\
C_q w_3(\xi) &= -w_3(\xi).
\end{aligned}
\tag{4.1}$$

The following easily obtained inner products will also be needed later.

$$\begin{aligned}
u_1(\tilde{q}) \cdot u_1(q) &= 1 - 2 \cos^2(\beta/2) \cos^2 \phi \\
w_1(\xi) \cdot u_1(q) &= \sqrt{1 - \cos^2(\beta/2) \cos^2 \phi} \\
w_2(\xi) \cdot u_1(q) &= -\cos(\beta/2) \cos \phi.
\end{aligned}
\tag{4.2}$$

Figure 7 shows (two copies of the fundamental domain of) the configuration manifold of the no-slip Sinai billiard. Here the billiard table is the complement of a circular scatterer in a two-dimensional torus and M is the cartesian product of the latter with a one-dimensional torus. Notice that there is a whole one-parameter family of initial conditions giving period-2 orbits, parametrized by the angle ϕ . We obtain infinitely many such families by choosing different pairs of fundamental domains.

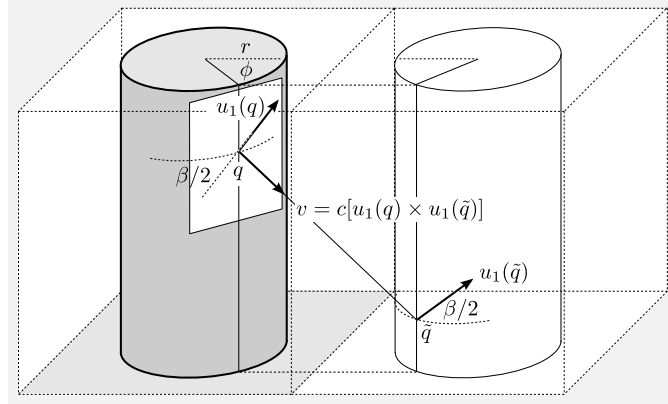


Figure 7: The figure shows two fundamental domains of the no-slip Sinai billiard and an initial velocity v of a periodic orbit with period 2. This trajectory lies in a one-parameter family of period-2 trajectories parametrized by the angle ϕ .

We will return to the no-slip Sinai billiard in Section 9.

5 THE DIFFERENTIAL OF THE NO-SLIP BILLIARD MAP

Mostly, in this section, we write $\langle u, v \rangle$ instead of $u \cdot v$ for the standard inner product of \mathbb{R}^3 . Let $q(s)$ be a smooth curve in ∂M such that $q(0) = q$ and $q'(0) = X \in T_q(\partial M)$. Define

$$\omega_q(X) := \left. \frac{d}{ds} \right|_{s=0} \sigma(q(0))^{-1} \sigma(q(s)) \in \mathfrak{so}(3)$$

where $\mathfrak{so}(3)$ is the space of antisymmetric 3×3 matrices (the Lie algebra of the rotation group) and $\sigma(q) := \sigma_q$ is the product frame. As e_1 is a parallel field and $\omega_q(X)$ is antisymmetric we have $\omega_q(X)_{ij} = 0$ except possibly for $(i, j) = (2, 3)$ and $(3, 2)$. Denoting by D_X directional derivative of vector fields along X at q ,

$$\omega_q(X)_{23} = \epsilon_2 \cdot \left[\left. \frac{d}{ds} \right|_{s=0} \sigma(q(0))^{-1} \sigma(q(s)) \epsilon_3 \right] = \langle e_2(q), D_X e_3 \rangle = \langle e_2(q), X \rangle \langle e_2(q), D_{e_2(q)} e_3 \rangle$$

since $D_{e_1} e_3 = 0$. The inner product $\kappa(q) := \langle e_2(q), D_{e_2(q)} e_3 \rangle$ is the geodesic curvature of the boundary of \mathcal{B} at \bar{q} , where \bar{q} is the base point of q in $\partial \mathcal{B}$. Thus

$$(5.1) \quad \omega_q(X) = \kappa(q) \langle e_2(q), X \rangle \mathcal{A}$$

where

$$\mathcal{A} = \begin{pmatrix} 0 & 0 & 0 \\ 0 & 0 & 1 \\ 0 & -1 & 0 \end{pmatrix}.$$

Given vector fields μ, ν , we define $\mu \odot \nu$ as the map

$$(5.2) \quad (q, v) \mapsto (\mu \odot \nu)_q v := \langle \mu_q, v \rangle \nu_q + \langle \nu_q, v \rangle \mu_q.$$

Lemma 5.1. *The directional derivative of C along $X \in T_q(\partial M)$ is*

$$D_X C = \kappa(q) \langle e_2(q), X \rangle \mathcal{O}_q$$

where $\mathcal{O}_q = \sigma_q \mathcal{O} \sigma_q^{-1}$,

$$\mathcal{O} := [\mathcal{A}, \mathcal{C}] = 2 \cos(\beta/2) \begin{pmatrix} 0 & 0 & \sin(\beta/2) \\ 0 & 0 & -\cos(\beta/2) \\ \sin(\beta/2) & -\cos(\beta/2) & 0 \end{pmatrix}$$

and \mathcal{C} was defined above in (2.3). Furthermore, $\mathcal{O}_q = 2 \cos(\beta/2) (u_1 \odot e_3)_q$ and

$$D_X C = 2 \cos(\beta/2) \kappa(q) \langle X, e_2 \rangle_q (u_1 \odot e_3)_q.$$

Proof. Notice that $0 = D_X I = D_X(\sigma^{-1} \sigma) = (D_X \sigma^{-1}) \sigma + \sigma^{-1} D_X \sigma$. Thus

$$D_X \sigma^{-1} = -\sigma^{-1} (D_X \sigma) \sigma^{-1}.$$

Therefore,

$$D_X C = (D_X \sigma) \mathcal{C} \sigma^{-1} + \sigma \mathcal{C} D_X \sigma^{-1} = \sigma [\sigma^{-1} D_X \sigma] \mathcal{C} \sigma^{-1} - \sigma \mathcal{C} [\sigma^{-1} D_X \sigma] \sigma^{-1} = \sigma [\omega(X), \mathcal{C}] \sigma^{-1}.$$

The first claimed expression for $D_X C$ is now a consequence of Equation 5.1. A simple computation also gives, for any given $v \in \mathbb{R}^3$,

$$(5.3) \quad \sigma(q) \mathcal{O} \sigma(q^{-1}) v = 2 \cos(\beta/2) (e_3 \odot u_1)_q v$$

yielding the second expression for $D_X C$. \square

It is convenient to define the following two projections. Let $\xi = (q, v) \in N^\pm$. The space $T_\xi N^\pm$ decomposes as a direct sum $T_\xi N^\pm = H_\xi \oplus V_\xi$ where

$$H_\xi = T_q N = \{X \in \mathbb{R}^3 : X \cdot e_3(q) = 0\} \text{ and } V_\xi = v^\perp = \{Y \in \mathbb{R}^3 : Y \cdot v = 0\}.$$

(Recall that $N := N^+$.) We refer to these as the *horizontal* and *vertical* subspaces of $T_\xi N^\pm$. We use the same symbols to denote the projections $H_\xi : \mathbb{R}^3 \rightarrow T_q(\partial M)$ and $V_\xi : \mathbb{R}^3 \rightarrow v^\perp$ defined by

$$H_\xi Z := Z - \frac{\langle Z, e_3(q) \rangle}{\langle v, e_3(q) \rangle} v, \quad V_\xi Z := Z - \langle Z, v \rangle v.$$

Notice that for $\xi = (q, v) \in N^\pm$ and $Z \in \mathbb{R}^3$

$$\langle e_2(q), H_\xi Z \rangle = \frac{\langle Z, e_2(q) \rangle \langle v, e_3(q) \rangle - \langle Z, e_3(q) \rangle \langle v, e_2(q) \rangle}{\langle v, e_3(q) \rangle} = \frac{\langle v \times e_1(q), Z \rangle}{\langle v, e_3(q) \rangle}.$$

Also observe that $v \times e_1 = |\bar{v}| w_2(\xi)$, where w_2 is the second vector in the wavefront frame (cf. Definition 3.1) and \bar{v} is the orthogonal projection of v to the plane perpendicular to e_1 . Thus, denoting by $\phi(\xi)$ the angle between \bar{v} and $e_3(q)$ (this is the same ϕ as in Figures 5, 6 and 7)

$$(5.4) \quad \langle e_2(q), H_\xi Z \rangle = \frac{1}{\cos \phi(\xi)} \langle w_2(\xi), Z \rangle.$$

Let $q \in \partial M$, $v = v_- \in N_q^-$, $v_+ := C_q v_- \in N_q^+$, $\xi = \xi_- = (q, v_-)$, $\xi_+ = (q, v_+)$. Define

$$(5.5) \quad \Lambda_\xi := V_{\xi_+} H_{\xi_-} : v_-^\perp \rightarrow v_+^\perp.$$

Clearly Λ_ξ is defined on all of \mathbb{R}^3 , not only on v_-^\perp , but we are particularly interested in its restriction to the latter subspace.

Let $\xi = (q, v)$ be a point contained in a neighborhood of N where T is defined and differentiable. Set $\tilde{\xi} = T(\xi)$. We wish to describe $dT_\xi : T_\xi N \rightarrow T_{\tilde{\xi}} N$. Let $\xi(s) = (q(s), v(s))$ be a differentiable curve in N with $\xi(0) = \xi$ and define

$$X := q'(0) \in T_q N, \quad Y := v'(0) \in v^\perp.$$

Then $\tilde{\xi}(s) = T(\xi(s)) = (\tilde{q}(s), \tilde{v}(s)) \in N$ where $\tilde{q}(s) = q(s) + t(s)v(s)$ and $\tilde{v}(s) = C_{\tilde{q}(s)} v(s)$. From the equality $\langle \tilde{q}'(0), e_3(\tilde{q}) \rangle = 0$ it follows that

$$t'(0) = - \frac{\langle X + tY, e_3(\tilde{q}) \rangle}{\langle v, e_3(\tilde{q}) \rangle}.$$

Consequently, $\tilde{X} := \tilde{q}'(0) \in T_{\tilde{q}}N$ and $\tilde{Y} := \tilde{v}'(0) \in \tilde{v}^\perp$ satisfy

$$\tilde{X} = X + tY - \frac{\langle X + tY, e_3(\tilde{q}) \rangle}{\langle v, e_3(\tilde{q}) \rangle} v = H_{\tilde{\xi}_-}(X + tY)$$

and

$$\tilde{Y} = C_{\tilde{q}}Y + \left[\frac{d}{ds} \Big|_{s=0} C_{\tilde{q}(s)} \right] v = C_{\tilde{q}}Y + \kappa(\tilde{q}) \langle e_2(\tilde{q}), \tilde{X} \rangle \mathcal{O}_{\tilde{q}} v$$

where we have used Lemma 5.1. From the same lemma,

$$\sigma(\tilde{q}) \mathcal{O} \sigma(\tilde{q})^{-1} v = -2 \cos(\beta/2) (\nu \odot u_1)_{\tilde{q}} v.$$

Thus

$$(5.6) \quad \begin{aligned} \tilde{X} &= H_{\tilde{\xi}_-}(X + tY) \\ \tilde{Y} &= C_{\tilde{q}}Y - 2 \cos(\beta/2) \kappa(\tilde{q}) \langle e_2(\tilde{q}), H_{\tilde{\xi}_-}(X + tY) \rangle (\nu \odot u_1)_{\tilde{q}} v. \end{aligned}$$

As already noted, $T_\xi N^+ = T_q(\partial M) \oplus v^\perp$. By using the projection $V_\xi : T_q(\partial M) \rightarrow v^\perp$ introduced earlier we may identify $T_\xi N^+$ with the sum $v^\perp \oplus v^\perp$. In this way dT_ξ is regarded as a map from $v^\perp \oplus v^\perp$ to $\tilde{v}^\perp \oplus \tilde{v}^\perp$.

Proposition 5.2. *Let $T : N \rightarrow N$ be the billiard map, $\xi = (q, v) \in N$ and $(\tilde{q}, \tilde{v}) = \tilde{\xi} = T(\xi)$, where $\tilde{q} = q + tv$, and $\tilde{v} = C_{\tilde{q}}v$. Under the identification of the tangent space $T_\xi N$ with $v^\perp \oplus v^\perp$ as indicated just above, we may regard the differential dT_ξ as a linear map from $v^\perp \oplus v^\perp$ to $\tilde{v}^\perp \oplus \tilde{v}^\perp$. Also recall from (5.4) the definition of $\Lambda_{\tilde{\xi}} : v^\perp \rightarrow \tilde{v}^\perp$. Then $dT_\xi : T_\xi N \rightarrow T_{\tilde{\xi}} N$ is given by*

$$\begin{pmatrix} X \\ Y \end{pmatrix} \mapsto \begin{pmatrix} \Lambda_{\tilde{\xi}}(X + tY) \\ C_{\tilde{q}}Y + 2 \cos(\beta/2) \kappa(\tilde{q}) \frac{\langle e_3 \odot u_1 \rangle_{\tilde{q}} v}{\cos \phi(\tilde{q}, v)} \langle w_2(\xi), X + tY \rangle \end{pmatrix}$$

where $\cos \phi(\tilde{q}, v) = \langle \bar{v}/|\bar{v}|, e_3(\tilde{q}) \rangle$ and \bar{v} is the orthogonal projection of v to e_1^\perp .

Proof. This is a consequence of the preceding remarks and definitions. \square

Corollary 5.1. *If $\xi = (q, v)$ is periodic of period 2, then $C_{\tilde{q}}v = -v$, $\langle v, u_1(\tilde{q}) \rangle = 0$, and the map of Proposition 5.2 reduces to*

$$\begin{pmatrix} X \\ Y \end{pmatrix} \mapsto \begin{pmatrix} X + tY \\ C_{\tilde{q}}Y + 2 \cos(\beta/2) \kappa(\tilde{q}) \frac{\cos \psi(\tilde{q}, v)}{\cos \phi(\tilde{q}, v)} \langle w_2(\xi), X + tY \rangle u_1(\tilde{q}) \end{pmatrix}.$$

where $\cos \psi(\tilde{q}, v) := \langle v, e_3(\tilde{q}) \rangle$, $\cos \phi(\tilde{q}, v) = \langle \bar{v}/|\bar{v}|, e_3(\tilde{q}) \rangle$.

Proof. Clearly, $C_{\tilde{q}}v = -v$, whence $\langle v, u_1(\tilde{q}) \rangle = 0$ and $(e_3 \odot u_1)_{\tilde{q}} v = \langle e_3(\tilde{q}), v \rangle u_1(\tilde{q})$. Also notice that $\Lambda_{\tilde{\xi}} Z = Z$ whenever $\langle Z, v \rangle = 0$. The corollary follows. \square

6 MEASURE INVARIANCE AND TIME REVERSIBILITY

It will be seen below that the no-slip billiard map does not preserve the natural symplectic form on N , so these mechanical systems are not Hamiltonian. Nevertheless, the canonical billiard measure derived from the symplectic form (the Liouville measure) is invariant and the system is time reversible, so some of the good features of Hamiltonian systems are still present. (See, for example, [14, 15] where a KAM theory is developed for reversible systems.)

Recall that the invertible map T is said to be *reversible* if there exists an involution \mathcal{R} such that

$$\mathcal{R} \circ T \circ \mathcal{R} = T^{-1}.$$

In order to see that the no-slip billiard map T is reversible we first define the following maps: $\Phi : (q, v) \mapsto (q + tv, v)$, where t is the time of free motion of the trajectory with initial state (q, v) , so that $q, q + tv \in \partial M$; the collision map $C : N \rightarrow N$ given by $C(q, v) = (q, C_q v)$; and the flip map $J : (q, v) \mapsto (q, -v)$ where $q \in \partial M$ and $v \in \mathbb{R}^3$. Recall that $T = C \circ \Phi$. Now set $\mathcal{R} := J \circ C = C \circ J$. It is clear (since C_q is an involution by Proposition 2.1) that $\mathcal{R}^2 = I$ and that $J \circ \Phi \circ J = \Phi^{-1}$. Therefore,

$$\mathcal{R} \circ T \circ \mathcal{R} = J \circ C^2 \circ \Phi \circ J \circ C = J \circ \Phi \circ J \circ C = \Phi^{-1} \circ C = (C \circ \Phi)^{-1} = T^{-1}.$$

Notice that if $L : V \rightarrow V$ is a reversible isomorphism of a vector space V with time reversal map $\mathcal{R} : V \rightarrow V$ (so that $\mathcal{R} \circ L \circ \mathcal{R} = L^{-1}$) then for any eigenvalue λ of L associated to eigenvector u , $1/\lambda$ is also an eigenvalue for the eigenvector $\mathcal{R}u$, as easily checked. These simple observations have the following useful corollary.

Proposition 6.1. *Let $\xi \in N$ be a periodic point of period k of the no-slip billiard system and let λ be an eigenvalue of the differential map $dT_\xi^k : T_\xi N \rightarrow T_\xi N$ corresponding to eigenvector u . Then $1/\lambda$ is also an eigenvalue of dT_ξ^k corresponding to eigenvector $\mathcal{R}u$, where \mathcal{R} is the composition of the collision map C and the flip map J . Furthermore, e_1 (see Definition 3.1) is always an eigenvector of dT_ξ and all its powers, corresponding to the eigenvalue 1.*

We now turn to invariance of the canonical measure. The canonical 1-form θ on N is defined by

$$\theta_\xi(U) := v \cdot X$$

for $\xi = (q, v) \in N$ and $U = (X, Y) \in T_q N \oplus v^\perp = T_\xi N$. Its differential $d\theta$ is a symplectic form on $N \cap \{v \in T_q(\partial M) : |v| = 1\}^c$ and $\Omega = d\theta \wedge d\theta$ is the canonical volume form on this same set. In terms of horizontal and vertical components of vectors in TN , the symplectic form is expressed as

$$d\theta(U_1, U_2) = Y_1 \cdot X_2 - Y_2 \cdot X_1$$

where $U_i = (X_i, Y_i)$. An elementary computation shows that the measure on N associated to Ω is given by

$$(6.1) \quad |\Omega_\xi| = v \cdot \nu(q) dA_{\partial M}(q) dA_N(v)$$

where $\nu(q) := e_3(q)$, $dA_{\partial M}(q)$ is the area measure on ∂M , and $dA_N(v)$ is the area measure on the hemisphere $N_q = \{v \in \mathbb{R}^3 : v \cdot \nu(q) > 0\}$.

Proposition 6.2. *The canonical 4-form Ω on N transforms under the no-slip billiard map as $T^*\Omega = -\Omega$. In particular, the associated measure $|\Omega|$, shown explicitly in Equation 6.1, is invariant under T .*

Proof. Let u be a vector field on ∂M and introduce the one-form θ^u on N given by

$$\theta_\xi^u(U) := (v \cdot u(q))(u(q) \cdot X)$$

for $\xi = (q, v)$ and $U = (X, Y)$. Taking u to be each of the vector fields u_1, u_2 we obtain the 1-forms θ^{u_1} and θ^{u_2} . As $v = (v \cdot u_1)u_1 + (v \cdot u_2)u_2 + (v \cdot \nu)\nu$ and $X \cdot \nu = 0$, we have

$$\theta = \theta^{u_1} + \theta^{u_2}.$$

The no-slip collision map C acts on $u = \theta^{u_i}$ as follows: For $U = (X, Y) \in T_q(\partial M) \oplus v^\perp$,

$$(C^*\theta^u)_\xi(U) = (C_q(v) \cdot u(q))(u(q) \cdot X) = (v \cdot C_q(u(q)))(u(q) \cdot X).$$

It follows that

$$C^*\theta^{u_1} = \theta^{u_1}, \quad C^*\theta^{u_2} = -\theta^{u_2}.$$

We now compute the differentials $d\theta^u$ for $u = u_1, u_2$. Observe that $\theta^u = f^u(\xi)(\pi^*u^b)$, where f^ξ is the function on N defined by $f^u(\xi) := v \cdot u(q)$ and π^*u^b is the pull-back under the projection map $\pi : N \rightarrow \partial M$ of the 1-form u^b on ∂M given by $u_q^b(X) = u(q) \cdot X$. Thus

$$d\theta^u = df^u \wedge (\pi^*u^b) + f^u \pi^* du^b.$$

A simple calculation gives

$$df_\xi^u(X, Y) = v \cdot (D_X u) + u(q) \cdot Y.$$

The vector field $u = u_i$ is parallel on ∂M . In fact, its derivative in direction $X \in T_q(\partial M)$ only has component in the normal direction, given by

$$D_X u = \kappa(q)(X \cdot e_2(q))(u(q) \cdot e_2(q))\nu(q).$$

Omitting the dependence on q , we have

$$df_\xi^u(X, Y) = \kappa(q)(X \cdot e_2)(u \cdot e_2)(v \cdot \nu) + u \cdot Y.$$

Another simple calculation gives

$$du_q^b(X_1, X_2) = (D_{X_1} u) \cdot X_2 - (D_{X_2} u) \cdot X_1 = 0$$

so $d\theta^u = df^u \wedge \pi^*u^b$. Explicitly,

$$d\theta^u(U_1, U_2) = (u \cdot Y_1)(u \cdot X_2) - (u \cdot Y_2)(u \cdot X_1) - \kappa(q)(v \cdot \nu)(u \cdot e_1)(u \cdot e_2)\omega(X_1, X_2)$$

where

$$\omega(X_1, X_2) := (e_1 \cdot X_1)(e_2 \cdot X_2) - (e_2 \cdot X_1)(e_1 \cdot X_2).$$

Notice that ω is the area form on ∂M . A convenient way to express $d\theta^u$ is as follows. Define the 1-form \tilde{u} on N by $\tilde{u}_\xi(U) = u(q) \cdot Y$, where $U = (X, Y) \in T_\xi N$, and the function $g^u(\xi) := -\kappa(q)(v \cdot \nu)(u \cdot e_1)(u \cdot e_2)$. These extra bits of notation now allow us to write

$$d\theta_\xi^u = g^u(\xi)(\pi^*\omega) + \tilde{u} \wedge (\pi^*u^\flat).$$

The main conclusion we wish to derive from these observations is that $d\theta^u \wedge d\theta^u = 0$. This is the case because, as $\dim(\partial M) = 2$, we must have $\omega^2 = 0$ and $\omega \wedge u^\flat = 0$. Therefore,

$$\Omega := d\theta \wedge d\theta = (d\theta^{u_1} + d\theta^{u_2}) \wedge (d\theta^{u_1} + d\theta^{u_2}) = 2d\theta^{u_1} \wedge d\theta^{u_2}.$$

Finally,

$$C^*\Omega = 2d(C^*\theta^{u_1}) \wedge d(C^*\theta^{u_2}) = -2d\theta^{u_1} \wedge d\theta^{u_2} = -\Omega.$$

The forms $d\theta$ and Ω are invariant under the geodesic flow and under the map it induces on N . As T is the composition of this map and C , the proposition is established. \square

7 WEDGE BILLIARDS

We set the following conventions for a wedge table with corner angle 2ϕ . See Figure 8. (This is the same ϕ that has appeared before in previous figures.) The boundary planes of the configuration manifold are denoted \mathcal{P}_1 and \mathcal{P}_2 . The orthonormal vectors of the constant product frame on plane \mathcal{P}_i are $e_{1,i}, e_{2,i}, e_{3,i} = \nu_i$ for $i = 1, 2$ where

$$\begin{aligned} e_{1,1} &= \begin{pmatrix} 0 \\ 0 \\ 1 \end{pmatrix}, & e_{2,1} &= \begin{pmatrix} \cos \phi \\ -\sin \phi \\ 0 \end{pmatrix}, & e_{3,1} &= \begin{pmatrix} \sin \phi \\ \cos \phi \\ 0 \end{pmatrix}, \\ e_{1,2} &= \begin{pmatrix} 0 \\ 0 \\ 1 \end{pmatrix}, & e_{2,2} &= -\begin{pmatrix} \cos \phi \\ \sin \phi \\ 0 \end{pmatrix}, & e_{3,2} &= \begin{pmatrix} \sin \phi \\ -\cos \phi \\ 0 \end{pmatrix}. \end{aligned}$$

Let $\sigma_i : \mathbb{R}^3 \rightarrow T_q \oplus \mathbb{R}\nu_i$ be the constant orthogonal map such that $\sigma_i \epsilon_j = e_{j,i}$, where ϵ_i , $i = 1, 2, 3$, is our notation for the standard basis vectors in \mathbb{R}^3 . Let

$$u_{1,i} = \sin(\beta/2)e_{1,i} - \cos(\beta/2)e_{2,i}, \quad u_{2,i} = \cos(\beta/2)e_{1,i} + \sin(\beta/2)e_{2,i}, \quad u_{3,i} = e_{3,i} = \nu_i$$

be the eigenvectors of the no-slip reflection map associated to the plane \mathcal{P}_i and set $\zeta_i \epsilon_j := u_{j,i}$. For easy reference we record their matrices here:

$$\zeta_i = \begin{pmatrix} (-1)^i \cos(\beta/2) \cos \phi & -(-1)^i \sin(\beta/2) \cos \phi & \sin \phi \\ \cos(\beta/2) \sin \phi & -\sin(\beta/2) \sin \phi & -(-1)^i \cos \phi \\ \sin(\beta/2) & \cos(\beta/2) & 0 \end{pmatrix}.$$

The initial velocity v for the period-2 trajectory points in the direction of $u_{1,2} \times u_{1,1}$ and is given by

$$v = \frac{1}{\sqrt{1 - \cos^2(\beta/2) \cos^2 \phi}} \begin{pmatrix} 0 \\ \sin(\beta/2) \\ \cos(\beta/2) \sin \phi \end{pmatrix}.$$

This periodic trajectory connects the points $q_1 \in \mathcal{P}_1$ and $q_2 \in \mathcal{P}_2$. Any such pair of points can be written as

$$q_1 = a \begin{pmatrix} \sin(\beta/2) \cos \phi \\ -\sin(\beta/2) \sin \phi \\ b - \cos(\beta/2) \sin^2 \phi \end{pmatrix}, \quad q_2 = a \begin{pmatrix} \sin(\beta/2) \cos \phi \\ \sin(\beta/2) \sin \phi \\ b + \cos(\beta/2) \sin^2 \phi \end{pmatrix}$$

where $a, b \in \mathbb{R}$, $a > 0$. In what follows we assume without loss of generality that $a = 1$ and $b = 0$. Thus

$$q_i = (\sin(\beta/2) \cos \phi, (-1)^i \sin(\beta/2) \sin \phi, (-1)^i \cos(\beta/2) \sin^2 \phi)^t.$$

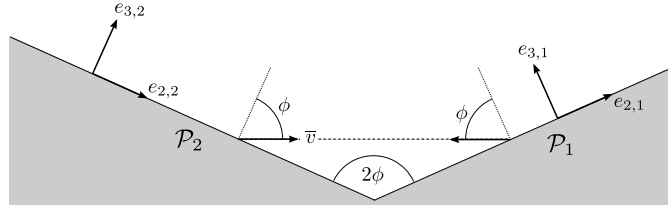


Figure 8: Some notation specific to the wedge billiard table. The \mathcal{P}_i are the half-plane components of the boundary of the configuration manifold.

Let $S_i^\pm = \{v \in \mathbb{R}^3 : |v| = 1, \pm v \cdot \nu_i > 0\}$. The collision maps $C_i : S_i^- \rightarrow S_i^+$, $i = 1, 2$ are given by the matrices

$$C_i = \sigma_i \mathcal{C} \sigma_i^{-1} = \zeta_i \begin{pmatrix} 1 & 0 & 0 \\ 0 & -1 & 0 \\ 0 & 0 & -1 \end{pmatrix} \zeta_i^{-1}$$

where \mathcal{C} was defined in 2.3. We now introduce coordinates on $\mathcal{P}_i \times S_i^+$ as follows. Let $S_+^2 = \{z \in \mathbb{R}^3 : |z| = 1, z_3 > 0\}$ and define $\Phi_i : \mathbb{R}^2 \times S_+^2 \rightarrow \mathcal{P}_i \times S_i^+$ by

$$\Phi_i(x, y) = (q_i + x_1 u_{1,i} + x_2 u_{2,i}, y_1 u_{1,i} + y_2 u_{2,i} + y_3 u_{3,i}).$$

Regarding $x \in \mathbb{R}^2$ as $(x, 0) \in \mathbb{R}^3$, we may then write

$$\Phi_i(x, y) = (q_i + \zeta_i x, \zeta_i y).$$

Clearly, the billiard map is not defined on all of $\bigcup_i \mathcal{P}_i \times S_i^+$ since those initial velocities not pointing towards the other plane will escape to infinity, but we are interested in the behavior of the map on a neighborhood of the periodic point $\xi_i = (q_i, v_i)$, $v_i = -(-1)^i v$. The question of interest here is whether some open neighborhood of ξ_i remains invariant under the billiard map. It is easily shown that the coordinates of the state ξ_i (of the period-2 orbit at the plane \mathcal{P}_i) are $\Phi_i^{-1}(\xi_i) = (0, y_i) \in \mathbb{R}^2 \times S_+^2$ where

$$y_i = \frac{1}{\sqrt{1 - \cos^2(\beta/2) \cos^2 \phi}} (0, (-1)^i \sin \phi, \sin(\beta/2) \cos \phi)^t$$

Let $T_i : \mathcal{D}_i \subset \mathbb{R}^2 \times S_+^2 \rightarrow \mathbb{R}^2 \times S_+^2$ be the billiard map restricted to $\mathcal{P}_i \times S_i^+$ expressed in the coordinate system defined by Φ_i . Thus

$$T_1 = \Phi_2^{-1} T \Phi_1, \quad T_2 = \Phi_1^{-1} T \Phi_2$$

on their domains \mathcal{D}_i . We now find the explicit form of T_i . Define $\bar{i} = \begin{cases} 1 & \text{if } i = 2 \\ 2 & \text{if } i = 1 \end{cases}$ and orthogonal matrices $A_i := \zeta_{\bar{i}}^{-1} \zeta_i$ and $S = \text{diag}(1, -1, -1)$, both in $SO(3)$. Also define

$$\alpha := 2 \sin \phi \sqrt{1 - \cos^2(\beta/2) \cos^2 \phi}.$$

Observe that $\zeta_{\bar{i}}^{-1} C_{\bar{i}} \zeta_i = S A_i$. It is easily shown that

$$q_i - q_{\bar{i}} = -\alpha v_i, \quad v_i = \zeta_i y_i, \quad A_i y_i = -y_{\bar{i}}, \quad S A_i y_i = y_{\bar{i}}.$$

In particular, $\zeta_{\bar{i}}^{-1}(q_i - q_{\bar{i}}) = -\alpha y_i$. Let $Q : \mathbb{R}^3 \times S_+^2 \rightarrow \mathbb{R}^2$ be defined by

$$Q(x, y) := x - \frac{x \cdot \epsilon_3}{y \cdot \epsilon_3} y.$$

Notice that $Q(x, y) \cdot \epsilon_3 = 0$. We now have

$$(7.1) \quad T_i : (x, y) \mapsto (Q(A_i(x - \gamma y_i), A_i y), S A_i y).$$

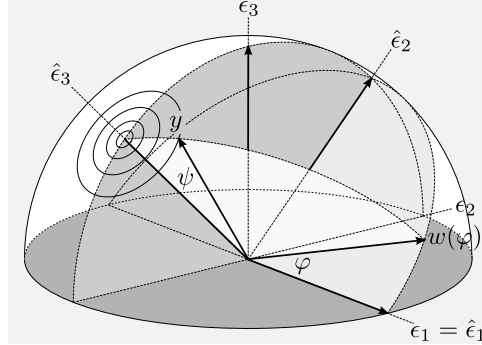


Figure 9: The velocity factor of orbits of the return billiard map $T_2 T_1$ in coordinate system Φ_1 lie in concentric circles with axis $y_1 = \hat{\epsilon}_3$. We use spherical coordinates φ and ψ relative to the axis $\hat{\epsilon}_3$ to represent the velocity $y \in S_+^2$. With respect to these coordinates, the return map sends $w(\varphi)$ to $w(\varphi + \theta)$, where θ is a function of the wedge angle α and the characteristic angle β of the no-slip reflection.

For easy reference we record

$$\alpha y_i = 2 \sin \phi \begin{pmatrix} 0 \\ (-1)^i \sin \phi \\ \sin(\beta/2) \cos \phi \end{pmatrix}, \quad S = \begin{pmatrix} 1 & 0 & 0 \\ 0 & -1 & 0 \\ 0 & 0 & -1 \end{pmatrix}$$

and

$$A_2 = A_1^t = \zeta_1^{-1} \zeta_2 = \begin{pmatrix} 1 - 2 \cos^2(\beta/2) \cos^2 \phi & -\sin \beta \cos^2 \phi & \cos(\beta/2) \sin(2\phi) \\ -\sin \beta \cos^2 \phi & 1 - 2 \sin^2(\beta/2) \cos^2 \phi & \sin(\beta/2) \sin(2\phi) \\ -\cos(\beta/2) \sin(2\phi) & -\sin(\beta/2) \sin(2\phi) & -\cos(2\phi) \end{pmatrix}.$$

Using the notation $[z]_3 := z \cdot \epsilon_3$ and elementary computations based on the above gives:

Proposition 7.1. *The return map in the coordinate system defined by Φ_1 has the form*

$$T_2 T_1(x, y) = (x + [A_1(x - \alpha y_1)]_3 V(y), SA_1^t SA_1 y)$$

where

$$V(y) = \frac{[y]_3 A_1^t SA_1 y - [A_1^t SA_1 y]_3 y}{[A_1 y]_3 [A_1^t SA_1 y]_3}.$$

This vector satisfies: $[V(y)]_3 = 0$ and $V(y_1) = 0$. In particular, $T_2 T_1(x, y_1) = (x, y_1)$ whenever (x, y_1) is in the domain of $T_2 T_1$.

In order to study this return map in a neighborhood of (x, y_1) we use spherical coordinates about the axis y_1 :

$$(7.2) \quad y = \cos \psi y_1 + \sin \psi \cos \varphi \hat{e}_1 + \sin \psi \sin \varphi \hat{e}_2$$

where

$$\hat{e}_1 := \epsilon_1, \quad \hat{e}_2 := \frac{1}{\sqrt{1 - \cos^2(\beta/2) \cos^2 \phi}} (\sin(\beta/2) \cos \phi \epsilon_2 + \sin \phi \epsilon_3), \quad \hat{e}_3 := y_1$$

form an orthonormal frame. See Figure 9. (Notice the typographical distinction between the corner angle ϕ of the wedge domain and the spherical coordinate φ .) Let

$$(X(x, \varphi, \psi), Y(x, \varphi, \psi)) := T_2 T_1(x, \cos \psi y_1 + \sin \psi \cos \varphi \hat{e}_1 + \sin \psi \sin \varphi \hat{e}_2)$$

and define

$$w := w(\varphi) := \cos \varphi \hat{e}_1 + \sin \varphi \hat{e}_2.$$

Thus we may write $y = \cos \psi (y_1 + \tan \psi w(\varphi))$. Since the rotation $S_2 := SA_1^t SA_1$ fixes y_1 , it acts on w as $S_2 w(\varphi) = w(\varphi + \theta)$ for some constant angle θ . It follows that

$$S_2 y = \cos \psi y_1 + \sin \psi w(\varphi + \theta).$$

The following proposition summarizes these observations and notations.

Proposition 7.2. *For points $y \in S_+^2$ in a neighborhood of y_1 we adopt spherical coordinates relative to the axis $y_1 = \hat{e}_3$, so that $y = \cos \psi (y_1 + \tan \psi w(\varphi))$ where*

$$w := w(\varphi) := \cos \varphi \hat{e}_1 + \sin \varphi \hat{e}_2.$$

See Figure 9. We also use the notations $[z]_3 := z \cdot \epsilon_3$, $S_1 := A_1^{-1} SA_1$, and $S_2 = SA_1^{-1} SA_1$. Let $R := T_2 T_1$ be the 2-step return map as defined above, whose domain contains a neighborhood of (x, y_1) for all $x \in \mathbb{R}^2$. Then $R(x, y_1) = (x, y_1)$ for all x and

$$R(x, y_1 + \tan \psi w(\varphi)) = (X, y_1 + \tan \psi S_2 w(\varphi)) = (X, \tan \psi w(\varphi + \theta))$$

for an angle θ , depending only on the wedge angle 2ϕ and the characteristic angle β of the no-slip reflection, such that

$$\begin{aligned}\cos \theta &= (S_2 \hat{e}_1) \cdot \hat{e}_1 = 1 - 8\delta^2 + 8\delta^4 \\ \sin \theta &= (S_2 \hat{e}_1) \cdot \hat{e}_2 = 4\delta(1 - 2\delta^2)\sqrt{1 - \delta^2}\end{aligned}$$

where $\delta := \cos(\beta/2) \cos \phi$. Writing $(X, \Phi, \Psi) = R(x, \varphi, \psi)$ we have

$$(7.3) \quad R: \begin{cases} X &= x + \tan \psi \frac{[A_1(x - \gamma y_1)]_3}{[y_1]_3} \frac{(I + S_1)w - \frac{[(I + S_1)w]_3 y_1}{[y_1]_3} + \tan \psi \frac{[w]_3 S_1 w - [S_1 w]_3 w}{[y_1]_3}}{1 - \tan \psi \left(\frac{[(A_1 + S_1)w]_3}{[y_1]_3} - \tan \psi \frac{[A_1 w]_3 [S_1 w]_3}{[y_1]_3^2} \right)} \\ \Phi &= \varphi + \theta \\ \Psi &= \psi \end{cases}$$

Denoting $\mu_1 := \zeta_1^{-1} \epsilon_3 \in \mathbb{R}^2$, we further have $X(x + s\mu_1, \varphi, \psi) = X(x, \varphi, \psi) + s\mu_1$.

Since ψ remains constant under iterations of the return map $R = T_2 T_1$, we regard ψ as a fixed parameter. We are interested in small values of $r := \tan \psi$. Notice that $[A_1 z]_3 := (A_1 z) \cdot \epsilon_3 = z \cdot (A_1^t \epsilon_3) = \mu_0 \cdot z$, where

$$\mu_0 := A_1^t \epsilon_3 = \begin{pmatrix} \cos(\beta/2) \sin(2\phi) \\ \sin(\beta/2) \sin(2\phi) \\ -\cos(2\phi) \end{pmatrix}.$$

Write $x_0 := \alpha y_1$, so

$$x_0 = 2 \sin \phi \begin{pmatrix} 0 \\ -\sin \phi \\ \sin(\beta/2) \cos \phi \end{pmatrix}.$$

Then the proposition shows that R has the form

$$(7.4) \quad R: (x, \varphi) \mapsto (X = x + \mu_0 \cdot (x - x_0) V_r(\varphi), \Phi = \varphi + \theta)$$

where the vector $V_r(\varphi)$ can be made arbitrarily (uniformly) small by choosing ψ (or $r = \tan \psi$) sufficiently close to 0. Observe from the explicit form

$$V_r(\varphi) = \frac{1}{[y_1]_3} \frac{r \left((I + S_1)w - \frac{[(I + S_1)w]_3 y_1}{[y_1]_3} \right) + r^2 \frac{[w]_3 S_1 w - [S_1 w]_3 w}{[y_1]_3}}{1 - r \frac{[(A_1 + S_1)w]_3}{[y_1]_3} + r^2 \frac{[A_1 w]_3 [S_1 w]_3}{[y_1]_3^2}}$$

that $V_r(\varphi) \cdot \epsilon_3 = 0$ so that X is indeed in \mathbb{R}^2 .

Proposition 7.3. *The quantity $1 + \mu_0 \cdot V_r(\varphi)$ satisfies the coboundary relation*

$$(7.5) \quad 1 + \mu_0 \cdot V_r(\varphi) = \frac{\rho(\varphi)}{\rho(\varphi + \theta)}$$

where

$$\rho(\varphi) = 1 + r \frac{\tan \phi}{\sin(\beta/2)} \sin \varphi.$$

In fact, the transformation R on the 3-dimensional space $\mathbb{R}^2 \times \mathbb{R}/(2\pi\mathbb{Z})$, obtained by fixing a value of ψ (hence of $r = \tan \psi$), leaves invariant the measure

$$d\mu = c \left(1 + r \frac{\tan \phi}{\sin(\beta/2)} \sin \phi \right) dA d\varphi$$

where c is a positive constant (only dependent on the fixed parameters β, ψ, ϕ) and A is the standard area measure on \mathbb{R}^2 .

Proof. The canonical invariant measure on $\mathbb{R}^2 \times S_+^2$ has the form $y \cdot \epsilon_3 dA dA_S$, where A_S is the area measure on S_+^2 . For a fixed value of ψ we obtain an invariant measure on $\mathbb{R}^2 \times S^1$ of the form $y \cdot \epsilon_3 dA d\varphi$. Using the form of y given by (7.2), one obtains

$$y \cdot \epsilon_3 = \frac{\cos \psi \cos \phi \sin(\beta/2)}{\sqrt{1 - \cos^2(\beta/2) \cos^2 \phi}} \left(1 + r \frac{\tan \phi}{\sin(\beta/2)} \sin \phi \right).$$

This shows that, up to a multiplicative constant, the invariant measure μ has the indicated form. Equation (7.5) is an easy consequence of the invariance of μ with respect to R . \square

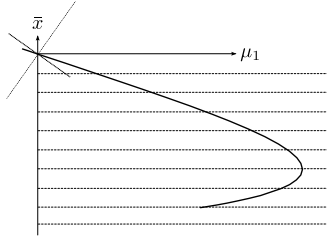


Figure 10: The map R sends fibers $x + \mathbb{R}\mu_1$ onto other such fibers preserving length. That is, $dR_{(x,\varphi)}\mu_1 = \mu_1$. The quotient is a measure preserving transformation on $\mathbb{R} \times \mathbb{T}^1$. The coordinate on the first factor of the quotient is $\bar{x} = x \cdot \mu_0$. The curve shown above is typical of the set to which orbits of R project in \mathbb{R}^2 .

By using the coordinate system $(\bar{x}, \bar{y}) \mapsto \bar{x}\mu_0 + \bar{y}\mu_1$ on \mathbb{R}^2 , the area measure is $dA = d\bar{x} d\bar{y}$ and, as observed at the end of Proposition 7.2, the transformation R maps the fibers of the projection $(\bar{x}, \bar{y}) \mapsto \bar{x}$ to fibers preserving the length measure on fibers. Thus we obtain a transformation \bar{R} on $\mathbb{R} \times S^1$ preserving the measure $d\bar{\mu}(\bar{x}, \varphi) = \rho(\varphi) d\bar{x} d\varphi$ where $\rho(\varphi)$ has the stated expression. Using the quotient coordinates $\bar{x} = x \cdot \mu_0$ and ϕ and writing $\bar{V}_r(\varphi) := V_r(\varphi) \cdot \mu_0$ we obtain

$$\bar{R}(\bar{x}, \phi) = ((1 + \bar{V}_r(\varphi))\bar{x} - \bar{x}_0 \bar{V}_r(\varphi), \phi + \theta).$$

In particular,

$$\bar{X} = \frac{\rho(\varphi)}{\rho(\varphi + \theta)} \bar{x} + \left(1 - \frac{\rho(\varphi)}{\rho(\varphi + \theta)} \right) \bar{x}_0.$$

The invariant measure is

$$d\bar{\mu}(\bar{x}, \varphi) = \rho(\varphi) d\bar{x} d\varphi$$

where $\rho(\varphi)$ is the density given in Proposition 7.3. It is now immediate that

$$\bar{R}^n(\bar{x}, \varphi) = \left(\frac{\rho(\varphi)}{\rho(\varphi + n\theta)} \bar{x} + \left(1 - \frac{\rho(\varphi)}{\rho(\varphi + n\theta)} \right) \bar{x}_0, \varphi + n\theta \right).$$

This shows that all the iterates of (\bar{x}, φ) remain uniformly close to the initial point for small values of ψ . Also notice that $(\zeta_1 \mu_0) \cdot e_{2,1} = \nu_2 \cdot e_{2,1} = \sin(2\phi) > 0$. This means that if \bar{x} remains bounded, the length coordinate along the base of \mathcal{P}_1 also must be similarly bounded. From this we conclude:

Corollary 7.1. *Assume the notation introduced at the beginning of this section. For all $q \in \mathcal{P}_i \setminus (\mathcal{P}_1 \cap \mathcal{P}_2)$, $i = 1, 2$, and any neighborhood \mathcal{V} of the period-2 state $(q, v_i) \in S_i^+$, there exists a small enough neighborhood $\mathcal{U} \subset \mathcal{V}$ of (q, v_i) the orbits of whose points remain in \mathcal{V} .*

Because any (bounded) polygonal billiard shape must have a corner with angle less than π , the following corollary holds.

Theorem 7.1. *Polygonal no-slip billiards cannot be ergodic for the canonical invariant measure.*

8 HIGHER ORDER PERIODIC ORBITS IN POLYGONS

The analysis of the previous section is based on the existence of period-2 orbits in wedge-shaped no-slip billiard tables. Existence of periodic orbits of higher periods is in general difficult to establish, although one such result for wedge domains will be indicated below in this section. We first point out a generalization of Corollary 7.1 to perturbations of periodic orbits in general polygon-shaped domains.

Figure 11 illustrates the type of stability implied by the following Theorem 8.1.

Theorem 8.1. *Periodic orbits in no-slip polygon-shaped billiard domains are locally stable. That is, given an initial state $\xi_0 = (q_0, v_0)$ for a period- n orbit in such a billiard system, and for any neighborhood \mathcal{V} of ξ_0 , there exists a small enough neighborhood $\mathcal{U} \subset \mathcal{V}$ of ξ the orbits of whose elements remain in \mathcal{V} .*

Proof. The idea is essentially the same as used in the proof of Proposition 7.3 and Corollary 7.1. We only indicate the outline. By a choice of convenient coordinates around the periodic point, it is possible to show that the n -th iterate of the billiard map T , denoted $R := T^n$, can be regarded as a map from an open subset of $\mathbb{R}^2 \times S^1$ into this latter set, having the form $R(x, \varphi) = (x_0 + A(\varphi)(x - x_0), \varphi + \theta)$ for a certain angle θ , where $A(\varphi)$ is a linear transformation independent of x . Rotation invariance implies that R must satisfy the invariance property $R(x + su, \varphi) = R(x, \varphi) + su$ for a vector $u \in \mathbb{R}^2$. From this we define a map \bar{R} on (a subset of) the quotient $\mathbb{R} \times S^1, \mathbb{R}^2/\mathbb{R}u$. Furthermore, denoting by (\bar{x}, φ) the coordinates in this quotient space, invariance of the canonical measure

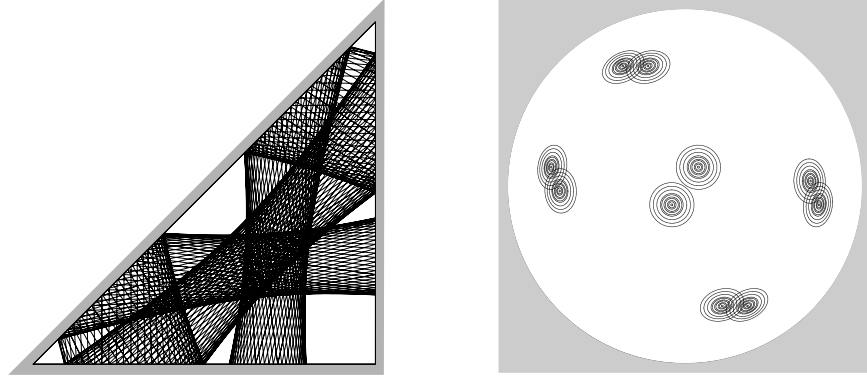


Figure 11: Projection to the plane of orbits in the neighborhood of a period-10 periodic orbit of a triangular no-slip billiard domain (left) showing typical stable behavior, along with the velocity phase portrait projections (right).

implies invariance of a measure μ on this quotient having the form $d\mu(\bar{x}, \varphi) = \rho(\varphi) d\bar{x} d\varphi$. Invariance is with respect to the quotient map $\bar{R}(\bar{x}, \varphi) = (\bar{x}_0 + a(\varphi)(\bar{x} - \bar{x}_0), \varphi + \theta)$ for some function $a(\varphi)$. This function must then take the form $a(\varphi) = \rho(\varphi)/\rho(\varphi + \theta)$. Iterates of \bar{R} will then behave like the corresponding map for the wedge domain, defined prior to Theorem 7.1. \square

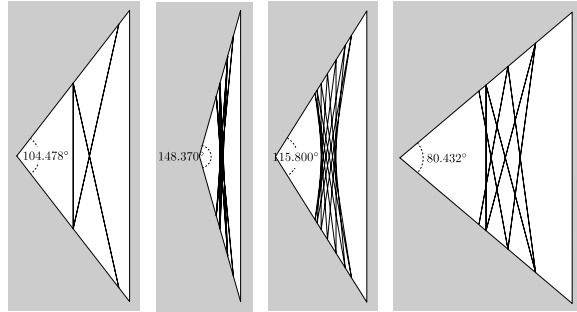


Figure 12: From left to right: projections to the plane of periodic orbits of periods 6, 14, 14, 14. (Bounded orbits in the same wedge domain are all periodic with the same period.) The rotation angle θ in each case is $2\pi p/q$ where $p/q = 1/3, 1/7, 2/7, 3/7$. Mass distribution of the disc particle is uniform.

We turn now to the question of existence of periodic orbits of higher (necessarily even) periods for wedge shapes. Clearly, a necessary condition is that the angle θ introduced in Proposition 7.2 (see also Figure 9) be rational. For orbits that do not eventually escape to infinity, this is also a sufficient condition, as a simple application of Poincaré recurrence

shows. (See [8].) Moreover, as θ is only a function of $\delta := \cos(\beta/2) \cos \phi$, which is given by (Proposition 7.2)

$$(8.1) \quad \cos \theta = 1 - 8\delta^2 + 8\delta^4$$

where β is the characteristic angle of the system (a function of the mass distribution on the disc) and 2ϕ is the corner angle of the wedge domain, if a higher order periodic orbit exists for a given δ , all bounded orbits have the same period.

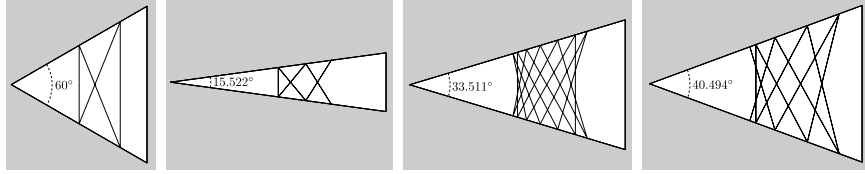


Figure 13: From left to right: projections of periodic orbits of periods 4, 10, 14, 18. The rotation angle θ in each case is $2\pi p/q$ where p/q is $1/2, 2/5, 3/7, 4/9$, respectively. Mass distribution is uniform.

We give a few examples for the uniform mass distribution, for which $\cos(\beta/2) = \sqrt{2/3}$. Solving 8.1 for $\cos \phi$, for $\theta = 2\pi p/q$, choosing first the negative square root, gives

$$(8.2) \quad \cos \phi_{p,q} := \frac{\sqrt{3}}{2} \sqrt{1 - \sqrt{\frac{1 + \cos(2\pi p/q)}{2}}}$$

A few examples are shown in Figure 12.

Notice that there are no restrictions on the values of p and q . The following proposition is a consequence of these remarks.

Theorem 8.2. *For any positive even integer n there exists a wedge domain for which the no-slip billiard has period- n orbits. More specifically, all bounded orbits of the no-slip billiard in a wedge domain with corner angle $\phi_{p,q}$ satisfying Equation 8.2 are periodic with period $2q$.*

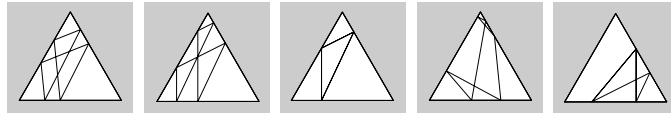


Figure 14: All orbits of an equilateral triangle no-slip billiard system are periodic with (not necessarily least) period equal to 4 or 6.

Solving 8.1 for $\cos \phi$, for $\theta = 2\pi p/q$, but choosing now the positive square root, gives

$$\cos \phi_{p,q} := \frac{\sqrt{3}}{2} \sqrt{1 + \sqrt{\frac{1 + \cos(2\pi p/q)}{2}}}.$$

This makes sense so long as $0.392 \approx \arccos(-7/9)/2\pi \leq p/q \leq 0.5$, which greatly restricts the choices of p and q . A few examples in this case are shown in Figure 13.

It is interesting to observe that all orbits of the equilateral triangle are periodic with period 4 or 6. (See Figure 14 and [8] for the proof.) We do not know of any other no-slip billiard domain all of whose orbits are periodic.

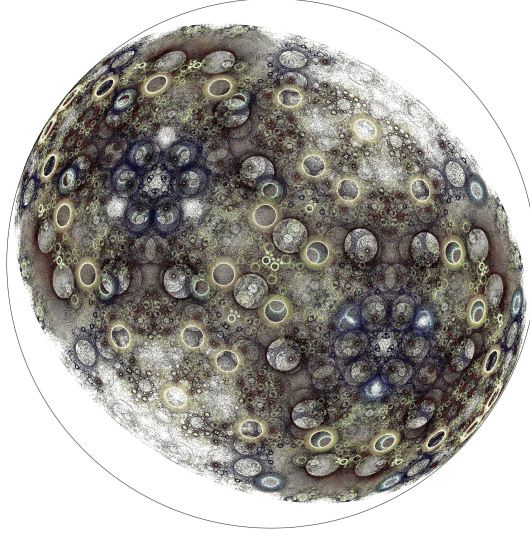


Figure 15: Velocity phase portrait of the no-slip billiard on a regular pentagon. Orbits all seem to lie in a stable neighborhood of some periodic orbit.

A final observation concerning polygonal no-slip billiards is suggested by plots of their velocity phase portraits. A typical such plot is shown in Figure 15. It is apparent that the orbits drawn all seem to lie on a stable neighborhood of some periodic orbit, and this pattern is seen at all scales that we have explored, but we do not yet have a clear topological dynamical description of this observation.

9 LINEAR STABILITY IN THE PRESENCE OF CURVATURE

We now turn to the problem of characterizing stability of period-2 orbits for no-slip billiard domains whose boundary may have non-zero geodesic curvature. Here we only address *linear* rather than local stability as we did before for polygonal billiards. In other words, we limit ourselves to the problem of determining when the differential of the billiard map dT_ξ at a period-2 collision state $\xi = (q, v)$ is elliptic or hyperbolic, and precise thresholds (where it is parabolic). To go from this information to local stability would require developing a KAM theory for no-slip billiards in the model of [14], something we do not do in this paper.

A simple but key observation is contained in the following lemma.

Lemma 9.1. *Let $\xi = (q, v)$ be periodic with period 2 for the no-slip billiard map and consider the differential $\mathcal{T} := dT_\xi^2 : v^\perp \oplus v^\perp \rightarrow v^\perp \oplus v^\perp$. Then either all the eigenvalues of \mathcal{T} are real, of the form $1, 1, r, 1/r$ or, if not all real, they are $1, 1, \lambda, \bar{\lambda}$ where $|\lambda| = 1$.*

Proof. This is a consequence of the following observations. First, we know that $T^*\Omega = -\Omega$, where Ω is the canonical symplectic form (cf. Section 6). Therefore, the product of the eigenvalues of \mathcal{T} counted with multiplicity is 1. The vector (e_1, w_1) , where e_1 is the first vector in the product frame and w_1 is the first vector in the wavefront frame, is an eigenvector for eigenvalue 1 of dT_ξ due to rotation symmetry, as already noted. If we regard dT_ξ as a self-map of $v^\perp \oplus v^\perp$ as in the corollary to Proposition 5.2 then we should use instead the vector (w_1, w_1) . (Recall that w_1 is collinear with the orthogonal projection of e_1 to v^\perp .) In addition, by reversibility of T , if λ is an eigenvalue of \mathcal{T} , then $1/\lambda$ is one also, and since \mathcal{T} is a real valued linear map, the complex conjugates $\bar{\lambda}$ and $1/\bar{\lambda}$ are also eigenvalues. As the dimension of the linear space is 4, if one of the eigenvalues, λ , is not real, it must be the case that $\lambda = 1/\bar{\lambda}$ and we are reduced to the case $1, 1, \lambda, \bar{\lambda}$ with $\lambda\bar{\lambda} = 1$. If all eigenvalues are real, and $r \neq 1$ is one eigenvalue, then we are reduced to the case $1, 1, r, 1/r$. \square

Corollary 9.1. *The period-2 point ξ is elliptic for $\mathcal{T} = dT_\xi^2$ if and only if $|\text{Tr}(\mathcal{T}) - 2| < 2$.*

To proceed, it is useful to express the differential map of Corollary 5.1 in somewhat different form. First observe, in the period-2 case (in which $\tilde{v} = -v$ and $v^\perp = \tilde{v}^\perp$), that

$$w_2(\xi) = -w_2(\tilde{\xi}) \text{ and } \frac{\cos \psi(\tilde{q}, v)}{\cos \phi(\tilde{q}, v)} = \frac{\cos \psi(\tilde{\xi})}{\cos \phi(\tilde{\xi})} = \frac{\cos \psi(\xi)}{\cos \phi(\xi)}.$$

(See Section 4.) Now define the rank-1 operator

$$\Theta_{\tilde{\xi}}(Z) := 2 \cos(\beta/2) \frac{\cos \psi(\tilde{\xi})}{\cos \phi(\tilde{\xi})} \langle w_2(\tilde{\xi}), Z \rangle u_1(\tilde{q}).$$

Then

$$(9.1) \quad dT_\xi \begin{pmatrix} X \\ Y \end{pmatrix} = \begin{pmatrix} I & tI \\ -\kappa(\tilde{q})\Theta_{\tilde{\xi}} & C_{\tilde{q}} - t\kappa(\tilde{q})\Theta_{\tilde{\xi}} \end{pmatrix} \begin{pmatrix} X \\ Y \end{pmatrix}.$$

When the geodesic curvature satisfies $\kappa(q) = \kappa(\tilde{q})$ we obtain a simplification in the criterion for ellipticity, as will be seen shortly. With this special case in mind we define the linear map R_ξ on v^\perp by $R_\xi w_i(\xi) = -(-1)^i w_i(\xi)$, $i = 1, 2$. Notice that $Ru_1(q) = u_1(\tilde{q})$. Then

$$R_{\tilde{\xi}} C_{\tilde{q}} = C_q R_\xi, \quad R_{\tilde{x}} \Theta_{\tilde{\xi}} = \Theta_\xi R_\xi.$$

The same notation R_ξ will be used for the map on $v^\perp \oplus v^\perp$ given by $(z_1, z_2) \mapsto (R_\xi z_1, R_\xi z_2)$. Notice that $R := R_\xi = R_{\tilde{\xi}}$ since $w_i(\tilde{\xi}) = -(-1)^i w_i(\xi)$. It follows that

$$(9.2) \quad RdT_\xi R = \begin{pmatrix} I & tI \\ -\kappa(\tilde{q})\Theta_\xi & C_q - t\kappa(\tilde{q})\Theta_\xi \end{pmatrix}.$$

In particular, when $\kappa(q) = \kappa(\tilde{q})$, we have $RdT_\xi R = dT_{\tilde{\xi}}$ and $dT_\xi^2 = (RdT_\xi)^2$. Therefore, rather than computing the trace of dT_ξ^2 , we need only consider the easier to compute trace of RdT_ξ . A straightforward calculation gives the trace of these maps, which we record in the next lemma.

Lemma 9.2. *Let $\xi = (q, v)$ have period 2 and set $\tilde{\xi} := T(\xi)$, $C := C_q$, $\Theta := \Theta_q$. Then*

$$\text{Tr}(dT_\xi^2) = \text{Tr}\{I + (CR)^2 - t(\kappa(q) + \kappa(\tilde{q}))[\Theta + (CR)(\Theta R)] + t^2\kappa(q)\kappa(\tilde{q})(\Theta R)^2\}.$$

When $\kappa := \kappa(\tilde{q}) = \kappa(q)$, we have $\text{Tr}(RdT_\xi) = \text{Tr}(CR + t\kappa\Theta)$.

Proof. These expressions follow easily given the above definitions and notations. \square

These traces can now be computed using Equations (4.1) and (4.2). The matrices expressing C, R, Θ in the wavefront basis of v^\perp are given as follows. For convenience we write

$$c := \cos(\beta/2), \quad c_\phi := \cos \phi, \quad c_\psi := \cos \psi, \quad \varrho := \sqrt{1 - \cos^2(\beta/2) \cos^2 \phi},$$

where $\phi = \phi(\xi)$ and $\psi = \psi(\xi)$ are defined in Corollary 5.1.

$$[C]_w = \begin{pmatrix} 1 - 2c^2c_\phi^2 & -2cc_\phi\varrho \\ -2cc_\phi\varrho & -1 + 2c^2c_\phi^2 \end{pmatrix}, \quad [R] = \begin{pmatrix} 1 & 0 \\ 0 & -1 \end{pmatrix}, \quad [\Theta]_w = 2c\frac{c_\psi}{c_\phi} \begin{pmatrix} 0 & \varrho \\ 0 & -cc_\phi \end{pmatrix}.$$

Let \bar{d} be the distance between the projections of q and \tilde{q} on plane the billiard table, \bar{v} the projection of v on the same plane and t , as before, the time between consecutive collisions. From $\cos \psi = \sin(\beta/2) \cos \phi / \sqrt{1 - \cos^2(\beta/2) \cos^2 \phi}$ it follows that $t \cos \psi = \cos \phi \bar{d}$. We then obtain

$$(9.3) \quad \text{Tr}(RdT_\xi) = \text{Tr}(CR) + t\kappa\text{Tr}(\Theta) = 2[1 - 2\cos^2(\beta/2)\cos^2\phi] - 2\kappa\bar{d}\cos^2(\beta/2)\cos\phi$$

and

$$(9.4) \quad \begin{aligned} \text{Tr}(dT_\xi^2) = 4 \Big\{ & [1 - 2\cos^2(\beta/2)\cos^2\phi]^2 \\ & - (\kappa(q) + \kappa(\tilde{q}))\cos^2(\beta/2)\cos\phi[1 - 2\cos^2(\beta/2)\cos^2\phi]\bar{d} \\ & + \kappa(q)\kappa(\tilde{q})\cos^4(\beta/2)\cos^2\phi\bar{d}^2 \Big\} \end{aligned}$$

Observe that in the special case in which $\kappa(q) = \kappa(\tilde{q})$ we have

$$\text{Tr}(dT_\xi^2) = \{2[1 - 2\cos^2(\beta/2)\cos^2\phi] - 2\kappa\cos^2(\beta/2)\cos\phi\bar{d}\}^2$$

Theorem 9.1. *Suppose that the billiard domain has a piecewise smooth boundary with at least one corner having inner angle less than π . Then, arbitrarily close to that corner point, the no-slip billiard has (linearly) elliptic period-2 orbits.*

Proof. Period-2 orbits exist arbitrarily close to the corners of a piecewise smooth billiard domain as Figure 16 makes clear. For period-2 orbits near a corner the above expression for $\text{Tr}(dT_\xi^2)$ gives for small \bar{d}

$$0 < \text{Tr}(dT_\xi^2) = 4[1 - 2\cos^2(\beta/2)\cos^2\phi]^2 + O(\bar{d}) < 4.$$

This implies that

$$|\mathrm{Tr}(dT_\xi^2) - 2| < 2$$

and the theorem follows from Corollary 9.1. \square

Theorem 9.1 (and numerical experiments) strongly suggests that such no-slip billiards will always admit small invariant open sets and thus cannot be ergodic with respect to the canonical billiard measure.

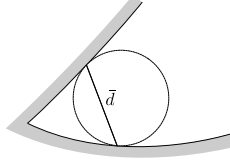


Figure 16: For a billiard domain with piecewise smooth boundary, arbitrarily near any corner with inner angle less than π , there are linearly stable period-2 orbits.

We illustrate numerically the transition between elliptic and hyperbolic in the special case of equal curvatures at q and \tilde{q} . Define $\zeta := \kappa \bar{d}$. When $\zeta > 0$ (equivalently, the curvature is positive), the critical value of ζ is

$$\zeta_0 = \frac{2 - 2 \cos^2(\beta/2) \cos^2 \phi}{\cos^2(\beta/2) \cos \phi}.$$

The condition for the periodic point to be elliptic is $\zeta > \zeta_0$. When $\zeta < 0$, the critical value of ζ is

$$\zeta_0 = -2 \cos \phi$$

and the condition for ellipticity is $|\zeta| < |\zeta_0|$.

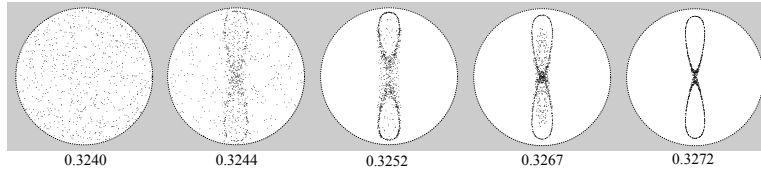


Figure 17: Velocity phase portraits of single orbits near the periodic orbit of the no-slip Sinai billiard corresponding to $\phi = 0$. The mass distribution is uniform. The numbers are the radius of the circular scatterer.

Consider the example of the no-slip Sinai billiard. (See Figures 4 and 7.) We examine small perturbations of the periodic orbit corresponding to the angle $\phi = 0$. Figure 17 suggests a transition from chaotic to more regular type of behavior for a radius between 0.32 and 0.33. In reality the critical radius for the $\phi = 0$ periodic orbits is exactly

1/3. So the observed numbers are smaller. We should bear in mind that the periodic points are not isolated, but are part of a family parametrized by ϕ . As ϕ increases, the critical parameter ζ_0 changes (for the uniform mass distribution, where $\cos^2(\beta/2) = 2/3$) according to the expression $\zeta_0 = (3 - \cos^2 \phi)/\cos \phi$. Given in terms of the radius of curvature, $\zeta = (1 - 2R \cos \phi)/R$. Solving for the critical R yields $R_0 = \frac{\cos \phi}{3}$. Thus for a period-2 trajectory having a small but non-zero ϕ , the critical radius is less than 1/3. It is then to be expected that the experimental critical value of R , for orbits closed to that having $\phi = 0$ will give numbers close to but less than 1/3. Moreover, as R_0 approaches 0 when ϕ approaches $\pi/2$, we obtain the following proposition which, together with experimental evidence indicates that the no-slip Sinai billiard is not ergodic.

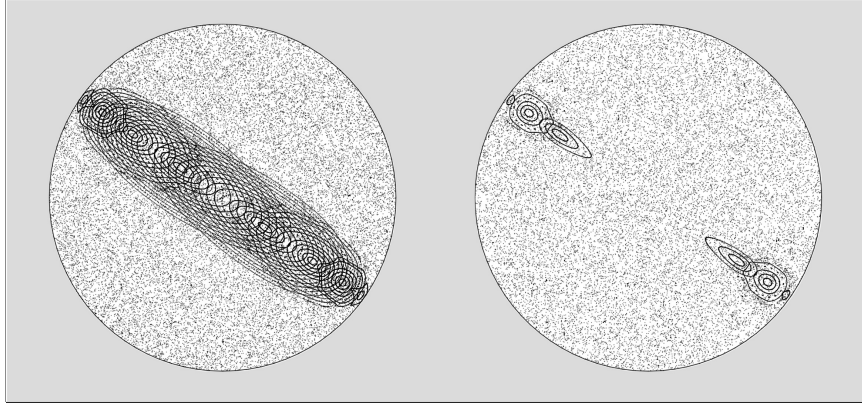


Figure 18: On the left: velocity phase portrait of the no-slip Sinai billiard with scatterer radius $R = 0.35$. Since this is greater than the transition value $R = 1/3$, the period-2 orbits parametrized by ϕ are all elliptic. On the right, $R = 0.32$ and ellipticity has been destroyed for orbits with smaller values of ϕ . No matter how small R is, elliptic orbits always exist for ϕ sufficiently close to $\pi/2$.

Proposition 9.3. *The no-slip Sinai billiard, for any choice of scatterer curvature, will contain (linearly) elliptic periodic trajectories of period 2.*

As another example, consider the family of billiard regions bounded by two symmetric arcs of circle depicted in Figure 19.

In this case, the critical transition from hyperbolic to elliptic, for the horizontal periodic orbit at middle height shown in the figure, happens for the disc. A transition behavior similar to that observed for the Sinai billiard seems to occur near the period-2 orbits shown in Figure 19. The number indicated below each velocity phase portrait is the angle of each circular arc. Thus, for example, the disc corresponds to angle π ; smaller angles give shapes like that on the left in Figure 19. The cut-off angle at which the indicated periodic orbit becomes elliptic is π . Notice, however, that the experimental value for this angle is greater than π . Just as in the Sinai billiard example, we should keep in mind

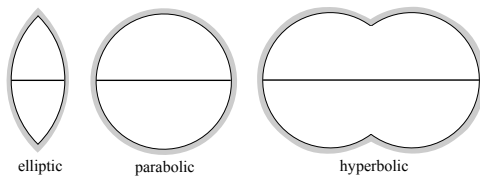


Figure 19: Family of focusing no-slip billiards.

that the periodic orbits are not isolated; in this case, the bias would be towards greater values of the angle.

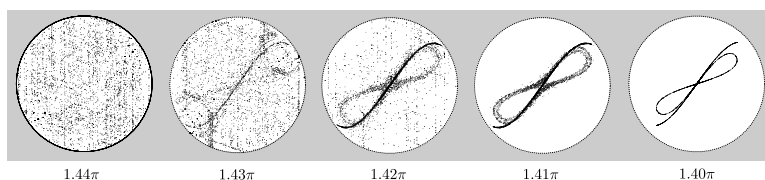


Figure 20: The indicated number is the angle of the circular cap. Each depicted orbit is a perturbation of the horizontal period-2 orbit at the middle height, as shown in Figure 19. Apparent chaotic behavior occurs for an angle much greater than π . This is expected since the parallel period-2 orbits remain linearly stable as the angle cap increases, up to a point.

REFERENCES

- [1] E. G. Altmann, T. Friedrich, A. E. Motter, H. Kantz, A. Richter, *Prevalence of marginally unstable periodic orbits in chaotic billiards*. Phys. Rev. E 77, 016205 (2008).
- [2] D.S. Broomhead, E. Gutkin, *The dynamics of billiards with no-slip collisions*. Physica D 67 (1993) 188-197.
- [3] L.A. Bunimovich, *The ergodic properties of certain billiards*. Funkt. Anal. Prilozh. 8 (1974) 73-74.
- [4] L. A. Bunimovich, *Mushrooms and other billiards with divided phase space*. Chaos, 11 (2001) 802-808.
- [5] N. Chernov, R. Markarian, *Chaotic billiards*. Mathematical Surveys and Monographs, V. 127, American Mathematical Society, 2006.
- [6] M. F. Correia, H. K. Zhang, *Stability and ergodicity of moon billiards*. Chaos, 25 083110 (2015).

- [7] C. Cox, R. Feres, *Differential geometry of rigid bodies collisions and non-standard billiards*. Discrete and Continuous Dynamical Systems-A, 33 (2016) no. 11, 6065–6099.
- [8] C. Cox, R. Feres, *No-slip billiards in dimension 2*. (arXiv:1602.01490)
- [9] C. Dettmann, O. Georgiou, *Open mushrooms: stickiness revisited*. Journal of Physics A: Mathematical and Theoretical, vol 44, (2011).
- [10] S. Kerckhoff, H. Masur, J. Smillie, *Ergodicity of billiard flows and quadratic differentials*. Ann. of Math. (2) 124 (1986), no. 2, 293-311.
- [11] I. Niven, *Irrational Numbers*, Wiley, 1956, p. 41.
- [12] Y. G. Sinai, *Dynamical systems with elastic reflections. Ergodic properties of dispersing billiards*. Uspehi Mat. Nauk 25 (1970), no. 2 (152), 141-192.
- [13] S. Tabachnikov, *Billiards*, in Panoramas et Synthèses 1, Société Mathématique de France, 1995.
- [14] M.B. Sevryuk, *Reversible Systems*, Lecture Notes in Mathematics 1211, Springer 1986.
- [15] M.B. Sevryuk, *Lower dimensional tori in reversible systems*. Chaos, 1 (1991) 160-167.
- [16] M. Wojtkowski, *The system of two spinning disks in the torus*. Physica D 71 (1994) 430-439.